Calcium-independent astrocytic lipid release modulates neuronal activity through Kv channels

Fushun Wang[1,2], Heather B. Bradshaw[3], Salvador Pena[4], Beata Jablonska[5], Julia Xavier[6], Sheng Gong[7], Baoman Li[1], Devin Chandler-Militello[1], Lane K. Bekar[8], and Nathan A. Smith[5,9,10*]

[1]Departments of Neurosurgery and Neurology, University of Rochester School of Medicine and Dentistry, Rochester, NY 14642, USA.
[2]Institute of Brain and Psychological Sciences, Sichuan Normal University, Chengdu, Sichuan 610060, China.
[3]Department of Psychological and Brain Sciences, Indiana University, Bloomington, IN 47405, USA
[4]Department of Pathology, University of Rochester School of Medicine and Dentistry, Rochester, NY 14642, USA
[5]Center for Neuroscience Research, Children's National Research Institute, Children's National Hospital, Washington DC 20010, USA.
[6]George Washington University, Washington DC 20052, USA.
[7]Department of Physiology and Biophysics, Case Western Reserve University School of Medicine, Cleveland, OH 44106, USA
[8]Department of Anatomy, Physiology, and Pharmacology, University of Saskatchewan, Saskatoon, SK S7N 5E5.
[9]George Washington University School of Medicine and Health Sciences, Washington DC 20052, USA.
[10]Lead Contact

*Correspondence should be addressed to Dr. Nathan Anthony Smith,
Email:nasmith2@childrensnational.org, Twitter: @SmithLab2018

ABSTRACT

Cumulative data point to a key role of Ca^{2+}-dependent gliotransmitter release as a modulator of neuronal networks. Here, we tested the hypothesis that astrocytes in response to agonist exposure also release lipid modulators through Ca^{2+}-independent phospholipase A_2 ($iPLA_2$) activity. We found that cultured rat astrocytes in response to agonist exposure, released Arachidonic Acid (AA) and/or its derivatives, including the endogenous cannabinoid, 2-arachidonoyl-sn-glycerol (2AG) and the prostaglandin E2 (PGE_2). Surprisingly, buffering of cytosolic Ca^{2+} was linked to a sharp increase in astrocytic lipid release. In addition, astrocytic release of PGE_2 enhanced mEPSPs by inhibiting the opening of neuronal Kv channels in acute brain slices. This study provides the first evidence for the existence of a Ca^{2+}-independent pathway for the release of PGE_2 from astrocytes and furthermore demonstrates a functional role for astrocytic lipid release in the modulation of synaptic activity.

INTRODUCTION

Comprising the majority weight of the adult brain, lipids are an essential component of the phospholipid bilayer and, of that, a large percentage are in the form of long chain polyunsaturated fatty acids (PUFA), mainly Arachidonic Acid (AA) and Docosahexaenoic Acid (DHA) (Sinclair, 1975). The liver is the major organ in the body for synthesis of AA, but the brain is also capable of producing AA and DHA from their precursor fatty acids, linoleic and linolenic acids (Dhopeshwarkar and Subramanian, 1976). Astrocytes play a pivotal role in this process. Through their vascular endfeet, astrocytes have prime access to incoming fatty acid precursors as they cross the blood brain barrier (BBB) and serve as the major site for processing essential fatty acids in the CNS (Moore, 1993). Astrocytes also play a key role in macroscopic distribution of lipids via perivascular glymphatic fluxes (Rangroo Thrane et al., 2013a; Plog and Nedergaard, 2018).

Lipids have gained much attention for their role as bioactive mediators in the CNS (Carta et al., 2014; Ledo et al., 2019). Numerous studies have focused on lipids in both functional hyperemia and synaptic activity. For instance, PGE_2 has been shown to be a potent vasodilator and vasoconstrictor in CNS blood flow regulation (Zonta et al., 2003; Takano et al., 2006; Gordon et al., 2007; Dabertrand et al., 2013; MacVicar and Newman, 2015; Czigler et al., 2019), as well as a regulator of membrane excitability in CA1 pyramidal neurons during synaptic activity (Chen and Bazan, 2005). Furthermore, AA and its derivatives are important secondary messengers that can modulate the activity of a variety of ion channels (Piomelli, 1993; Meves, 1994; Horimoto et al., 1997; Boland and Drzewiecki, 2008; Cordero-Morales and Vasquez, 2018). For example, the endocannabinoid, 2AG can suppress neurotransmitter release from the presynaptic membrane through the activation of cannabinoid receptor 1 (CB1) (Fride, 2002; Hashimotodani et al., 2007; Smith et al., 2019). In addition, PGE_2 has been shown to suppress Kv current in sensory neurons (Nicol et al., 1997; Evans et al., 1999), whereas AA suppresses Kv channels in the soma or dendrites of pyramidal neurons, and therefore, broadens presynaptic action potentials (Carta et al., 2014) and enhances EPSPs (Ramakers and Storm, 2002). However, these studies focused

on neuronal lipid release effects on synaptic activity and paid little or no attention to the fact that astrocytic lipid mediators via receptor-mediated pathways may also influence synaptic activity. Given that the majority of AA, DHA, and other lipids present in the extracellular fluid are produced by astrocytes (Moore et al., 1991), it is crucial to establish whether astrocytic lipid release actively modulates synaptic activity.

In culture, astrocytes can release AA in a $cPLA_2$ Ca^{2+}-dependent pathway upon activation of metabotropic glutamate and P2Y purine receptors (Bruner and Murphy, 1990; Stella et al., 1994; Stella et al., 1997; Chen and Chen, 1998). In addition, astrocytes also express the Ca^{2+}-independent PLA_2 ($iPLA_2$)(Sun et al., 2005). This PLA_2 isoform, like $cPLA_2$, is activated by the G-protein βγ subunit ($iPLA_2$) (Jelsema and Axelrod, 1987; Murayama et al., 1990; van Tol-Steye et al., 1999), but does not require Ca^{2+} or PKC phosphorylation for activation (Winstead et al., 2000). $iPLA_2$ has also been shown to release AA and DHA upon receptor stimulation in numerous cell types (Gross et al., 1993; Portilla et al., 1994; Akiba et al., 1998; Seegers et al., 2002; Tay and Melendez, 2004). However, to our knowledge, the role of $iPLA_2$ has yet to be fully explored in astrocytes.

Previous work in our lab and many others had demonstrated that astrocytes are capable of releasing gliotransmitters upon agonist stimulation. However, the question of whether astrocytes play a significant role in modulating synaptic activity is still controversial. Recent studies with genetically encoded calcium indicators enabled us to identify localized Ca^{2+} signals within fine processes, and have confirmed Ca^{2+}-dependent astrocytic effects on synaptic activity (Yu et al., 2018). However, the existence of Ca^{2+}-independent lipid signaling in astrocytes is still not clear. In this study, we assessed the existence of Ca^{2+}-independent lipid signaling in astrocytes and asked whether astrocytic lipid release can modulate synaptic transmission. Our analysis showed that upon Ca^{2+} chelation and receptor stimulation astrocytes can release lipids through $iPLA_2$ activation and that these lipids potentiate synaptic activity. These observations expand our understanding of how astrocytes can shape rapid synaptic events.

MATERIALS and METHODS

Culture

Cultured neocortical astrocytes were prepared from 1 to 2 day old Wistar rat pups (Taconic Farms, Inc.) of either sex as previously described (Lin et al., 1998). Briefly, cerebral cortices were dissected, and meninges were removed. The tissue was washed 3 times in Hanks' balanced salt solution without Ca^{2+}. Once washed, the tissue was triturated, filtered through 70 μm nylon mesh and then centrifuged. The pellet was resuspended in 10 % fetal bovine serum in Dulbecco's modified Eagle's medium (DMEM)/F12 containing penicillin (100 IU ml^{1}) and streptomycin (100 μg ml^{-1}), and transferred to culture flasks. Cells were maintained at 37˚C in an incubator containing humidified air and 5% CO_2. Medium was changed after 24 hrs and twice a week thereafter. More than 95% of the cells stained positive for GFAP. When the cells became confluent, they were rinsed two times in Hanks' balanced salt solution without Ca^{2+}, suspended in 0.05 % trypsin-containing solution for 1 min, resuspended in DMEM/F12, centrifuged to remove trypsin, and then plated in 24-well plates. Experiments were performed when the cells were 95% confluent.

Viral Vectors and Viral Transductions

Viral vectors driving GFAP cyto-GCaMP6f (Baljit S. Khakh) were obtained from the University of Pennsylvania Vector Core (AAV 2/5 serotype). Secondary rat astrocytic cultures were transduced with AAV GFAP cyto-GCaMP6f. After transduction, the cultures were incubated at 37˚C for 5 days prior to Ca^{2+} imaging experiments.

Ca^{2+} imaging

Cultured cells in 24-well plates were transduced with AAV GFAP cyto-GCaMP6f and incubated with various pharmacological agents for 30 minutes at 37˚C. Using confocal microscopy (Olympus FV500), calcium wave activity was evoked by adding equal volume of medium containing 100μM of ATP to each well. Relative increases in fluorescence signal evoked by agonist exposure over baseline fluoresce (ΔF/F) were calculated as previously described (Nedergaard, 1994; Smith et al., 2018).

Radiolabeling and Assessment of AA Release

Confluent rat astrocytic cultures were incubated with 100nCi ^{3}H-AA overnight prior to experiments. The cells were washed three times with serum-free medium. After washes, the cells were allowed to recover for 20 minutes. Before stimulation with 100 μM of ATP, the cells were incubated with appropriate inhibitors for 10 to 12 minutes. Aliquots of medium were taken 15 minutes after stimulation and ^{3}H-AA and/or its derivatives were measured by liquid scintillation counting.

HPLC/MS/MS analysis of lipids

Confluent rat astrocytes were washed with serum-free media and then allowed to recover for 1 hr in serum-free media. At this time cells were either incubated with vehicle or 20 μM CPA for 15 minutes and then challenged with 100 μM of ATP or vehicle for 15 minutes in the same protocol as the above radiolabeled experiments. Media was then removed and retained, 2 ml of HPLC-grade methanol was added to the flask for 5 minutes, removed and retained. An additional 2 ml of HPLC-grade methanol was added, cells were scraped and then this mixture was added to the previously two retained fractions. 200 pM deuterium-labeled standards were added, then samples were centrifuged at 19,000 x g in 24C. Lipids in the eluent were partially purified on 500mg C18 Bond Elut solid phase extraction columns (Varian), concentrated into methanolic fractions of 40%, 60%, 85%, and 100%, then analyzed using HPLC/MS/MS (Shimadzu SCL10Avp-Wilmington, DE, USA; API 3000 Applied Biosystems/MDS SCIEX, Foster city, CA, USA) as previously described (Leishman et al., 2018). Over 50 lipids were targeted in these screens including 40 lipoamines, 3 acyl glycerols, 2 free fatty acids, and 2 prostaglandins. It was determined in pilot studies that the signal detection of lipids in the media was too low for analysis of media alone; however, the signal with both the media and cells was more than sufficient to perform a large-scale analysis; therefore, the media and the cells were combined before the lipid extraction as outlined above.

PGE_2 Release Assessment via PGE_2 Immunoassay

Confluent rat astrocytic cultures were washed 3 times with serum-free medium. After washes, the cells were allowed to recover for 20 minutes. Before stimulation with 100 μM of ATP, the cells

were incubated with appropriate inhibitors for 10 to 12 minutes. Aliquots of medium were taken 15 minutes after stimulation and measured using a PGE_2 Enzyme Immunoassay Kit from Cayman Chemicals following the manufacturer's manual.

Western Blot

Samples harvested from 24-well plates were separated by SDS-PAGE and transferred to nitrocellulose. Membranes were blocked with Tris-buffered saline containing 0.05% (wt/vol) Tween 20 and 5% nonfat dry milk. The primary antibodies were anti-iPLA2 (Sigma, St. Louis, MO), anti-β-actin (Cell Signaling, Danvers, MA), at 1:1000 to 1:2000 dilutions in blocking buffer. Detection of chemiluminescence from horseradish peroxidase-linked secondary antibodies was performed using the ChemiDoc™ XRS+ System and running Image Lab™ software.

Isolation of human fetal astrocytes

Human fetal forebrain tissues were obtained from second-trimester aborted fetuses of 20 weeks gestational age. Tissues were obtained from aborted fetuses, with informed consent and tissue donation approval from the mothers, under protocols approved by the Research Subjects Review Board of the University of Rochester Medical Center. No patient identifiers were made available to or known by the investigators; no known karyotypic abnormalities were included. The forebrain tissue samples were collected and washed 2-3 times with sterile Hank's balanced salt solution with Ca^{2+}/Mg^{2+} ($HBSS^{+/+}$). The cortical plate region (CTX) of fetal forebrain was dissected and separated from the ventricular zone/subventricular zone (VZ/SVZ) portion. The CTX was then dissociated with papain as previously described (Keyoung et al., 2001). The cells were resuspended at 2-4 x 10^6 cells/ml in DMEM/F12 supplemented with N2, 0.5 % FBS and 10 ng/ml bFGF and plated in suspension culture dishes. The day after dissociation, cortical cells were recovered and subjected to magnetic activated cell sorting (MACS) for purification of the astrocyte progenitor population. Briefly, the recovered cells were incubated with CD44 microbeads as per the manufacturer's recommendations (Miltenyi Biotech). The cells were then washed, resuspended in Miltenyi Washing buffer and bound to a magnetic column (Miltenyi Biotech). The

bound CD44+ astrocyte progenitor cells were eluted, collected and then washed with DMEM/F12. The purified human fetal astrocyte progenitors were cultured in DMEM/F12 supplemented with N2 and 5% characterized FBS to further differentiate them. To prepare culture dishes for PGE2 immunoassays or immunocytochemistry, the fetal cortical astrocytes were dissociated with TrypLE (Invitrogen) into single cells and then plated onto poly-L-ornithine/laminin coated 24-well plates (50,000 cells per well).

shRNA Lentiviral knockdown of $iPLA_2$ in astrocytes

Rat astrocytes cultures were plated in a 24-well plate and grown to approximately 50% confluency. According to the manufacturer's instructions with modifications, the cultures were transduced overnight by adding either group VI $iPLA_2$ shRNA (r) lentiviral particles (sc-270117-V) or control shRNA lentiviral particles-A (sc-108080) directly to the culture medium containing polybrene (sc-134220) (all from Santa Cruz Biotechnology, Santa Cruz). 24 hrs after transfection, the culture medium was removed and fresh culture medium without polybrene was added. Experiments and western blot analysis were performed 7 days after transduction.

Acute Hippocampal Slice preparation and Electrophysiology

Unless otherwise noted, 15-21 day old C57BL/6 (Charles River, Wilmington, MA), $MrgA1^{+/-}$ transgenic, and littermate control $MrgA1^{-/-}$ pups (courtesy of Dr. Ken McCarthy) (Fiacco et al., 2007) of either sex were used for preparation of hippocampal slices as previously described (Wang et al., 2012). The pups were anesthetized in a closed chamber with isoflurane (1.5%), and decapitated. The brains were rapidly removed and immersed in ice-cold cutting solution that contained (in mM): 230 sucrose, 2.5 KCl, 0.5 $CaCl_2$, 10 $MgCl_2$, 26 $NaHCO_3$, 1.25 NaH_2PO_4, and 10 glucose, pH=7.2-7.4. Coronal slices (400 μm) were cut using a vibratome (Vibratome Company, St. Louis) and transferred to oxygenated artificial cerebrospinal fluid (aCSF) that contained (in mM): 126 NaCl, 4 KCl, 2 $CaCl_2$, 1 $MgCl_2$, 26 $NaHCO_3$, 1.25 NaH_2PO_4, and 10 glucose, pH = 7.2-7.4, osmolarity = 310 mOsm. Slices were incubated in aCSF for 1-5 hours at room temperature before recording. Experiments were performed at room temperature (21-23

˚C). During the recordings, the slices were placed in a perfusion chamber and superfused with aCSF gassed with 5% CO_2 and 95% O_2 at room temperature. Cells were visualized with a 40X water-immersion objective and differential inference contrast (DIC) optics (BX51 upright microscope, Olympus Optical, New York, NY). Patch electrodes were fabricated from filament thin-wall glass (World Precision Instruments) on a vertical puller; resistance of the pipette was around 6-9 MΩ with intracellular pipette solution added. The pipette solution contained (in mM) 140 K-gluconate, 5 Na-phosphocreatine, 2 $MgCl_2$, 10 HEPES, 4 Mg-ATP, 0.3 Na-GTP (pH adjusted to 7.2 with KOH). Current-voltage relationship (I-V curve) of voltage-gated potassium currents were recorded under voltage-clamp using an AxoPatch MultiClamp 700B amplifier (Axon Instruments, Forster City, CA). When measuring outward currents, QX314 (0.5 mM) was added to the pipette solution to block Na^+ currents. For recordings of miniature EPSPs (mEPSPs) 0.5 μM TTX was added in the aCSF. The junction potential between the patch pipette and bath solution was zeroed before forming a giga-seal. Patches with seal resistances of less than 1 GΩ were rejected. Data were low-pass filtered at 2 kHz and digitized at 10 kHz with a Digidata 1440 interface controlled by pClamp Software (Molecular Devices, Union City, CA).

Pharmacological agents used in cultures and slice experiments

Adenosine 5 -triphosphate (ATP, 100 μM); Cyclopiazonic acid (CPA, 20 μM); *trans*- (1S, 3R)-1-Amino-1, 3-cyclopentanedicarboxylic acid (*t*-ACPD, 100 μM); (±)-α-Amino-3-hydroxy-5-methylisoxazole-4-propionic acid hydrobromide ((±)-AMPA, 100 μM); Prostaglandin E_2 (PGE_2, 50 μM, Tocris); Phe-Met-Arg-Phe amide (FMRF, 15 μM); Thr-Phe-Leu-Leu-Arg-NH_2 (TFLLR-NH_2, 30 μM, Tocris); N-Acetyl-Asp-Glu (NAAG, 100 μM); (1*R*, 4*R*, 5*S*, 6*R*)-4-Amino-2-oxabicyclo [3.1.0] hexane-4,6-dicarboxylic acid disodium salt (LY379268, 100 μM, Tocris); Calmidazolium chloride (CMZ, 2 μM, Tocris); Methyl arachidonyl fluorophosphonate (MAFP, 10 μM); Bromoenol lactone (Bel, 10 μM); Arachidonic Acid (AA, 50 μM); *N*-(2,6-Dimethylphenylcarbamoylmethyl) triethylammonium chloride (QX314, 1mM, Tocris); 4-(4-,9-Diethoxy-1,3-dihydro-1-oxo-2*H*-benz[f]isoindol-2-yl)-*N*-(phenylsulfonyl) benzeneacetamide (GW627368X 3 μM, Tocris); 6-

Isopropoxy-9-xanthone-2-carboxylic acid (AH6809, 10 μM, Tocris); *N*-(Piperidin-1-yl)-5-(4-iodophenyl)-1-(2,4-dichlorophenyl)-4-methyl-1*H*-pyrazole-3-carboxamide (AM251, 5 μM, Tocris); Tetrodotoxin (TTX, 0.5 μM, Tocris); 1,2-Bis(2-aminophenoxy)ethane-*N*,*N*,*N*',*N*'-tetraacetic acid (Bapta, 50 μM, Tocris); and 1,2-*Bis*(2-aminophenoxy)ethane-*N*,*N*,*N*',*N*'-tetra-acetic acid tetrakis (acetoxymethylester) (BAPTA-AM, 20 μM). All chemicals were from Sigma unless otherwise noted.

Statistical analysis of data

Statistical significance was evaluated by one-way ANOVA and Post Hoc Tests (Tukey and Dunn) using Prism software and deemed significant when $P<0.05$ for ^{3}H-AA and PGE_2 assay experiments. Normality of the data was evaluated with Shapiro-Wilk test with a = 0.05. For electrophysiology experiments, significance was determined by paired or unpaired t-tests or Tukey-Kramer post hoc multiple comparison tests. HPLC/MS/MS lipidomics data were analyzed with ANOVA and Fishers LSD post-hoc using SPSS when $P<0.05$ or $P<0.10$. All results are reported as mean ± s.e.m.

RESULTS

GPCR-mediated Ca^{2+}-independent release of ^{3}H-AA and its derivatives from astrocytic cultures

We first assessed the efficiency by which preloading with inhibitor of the endoplasmic reticulum (ER) Ca^{2+} pump cyclopiazonic acid (CPA) (20 μM) or the cytosolic Ca^{2+} chelator 1,2-bis(o-aminophenoxy)ethane-N,N,N′,N′-tetraacetic acid (acetoxymethyl ester) (BAPTA-AM) (20 μM) blocked ATP (100 μM) induced cytosolic Ca^{2+} in cultured rat astrocytes. Imaging cytosolic Ca^{2+} (AAV GFAP cyto-GCaMP6f) showed that the purine agonist ATP (100 μM) induced a prompt increase in Ca^{2+} that was completely blocked in CPA and BAPTA loaded cultures, whereas 10 μM Methylarachidonyl Fluorophosphates (MAFP), a nonspecific inhibitor of both $cPLA_2$ and $iPLA_2$ or

10 μM of Bromoenol Lactone (Bel) (Cornell-Bell et al.), a specific inhibitor of $iPLA_2$ did not affect ATP induced Ca^{2+} rises in cultures **(Figure 1A-B)**.

As a broad-based approach to AA-specific lipidomics, Ca^{2+}-independent release of AA and/or its derivatives was performed using a ^{3}H-AA assay **(Figure 1C)**. Cultured rat astrocytes were pre-incubated overnight with ^{3}H-AA, providing sufficient time for ^{3}H-AA to be incorporated in multiple biosynthetic and metabolic pathways including membrane phospholipids, which are precursors for endocannabinoids, and related lipids that are themselves precursors to AA release (Chen and Chen, 1998; Strokin et al., 2003). Therefore, this assay serves to determine if any AA derivatives (precursors or metabolites) from the ^{3}H-AA that was incorporated into the cell are being released and all such lipids species will be referred to hereafter as ^{3}H-AA labeled metabolites. ATP on its own failed to induce the release of ^{3}H-AA that was within the level of detection **(Figure 1D)**; however, in cultures pretreated for 10 to 12 minutes with CPA or BAPTA-AM, ATP evoked a robust increase in the release of ^{3}H-AA, whereas CPA alone had no effect **(Figure 1D)**. Similarly, we found that upon stimulation with a combination of tACPD (100 μM), an mGluR agonist, and AMPA (100 μM), an ionotropic GluR agonist, we observe a significant release of ^{3}H-AA when cytosolic Ca^{2+} was blocked with CPA, but not in cultures without CPA pretreatment **(Figure 1E)**. These observations confirm that rat astrocytes can release AA derivatives, key precursors of bioactive eicosanoids (Strokin et al., 2003; Rosenegger et al., 2015), but that AA release is, surprisingly, inhibited by increases in cytosolic Ca^{2+}.

$iPLA_2$ activity is essential for Ca^{2+} independent release of AA-derived lipids.

To explore the mechanism of Ca^{2+}-independent release of ^{3}H-AA, we next evaluated whether inhibition of the Ca^{2+}-sensitive $cPLA_2$ or alternatively of the Ca^{2+}-insensitive $iPLA_2$ enzymes would reduce ^{3}H-AA release. Astrocytes were pretreated with 10 μM of MAFP or 10 μM of BEL. MAFP significantly decreased the release of ^{3}H-AA in response to ATP in cultures exposed to CPA **(Figure 1F)**. Similarly, BEL suppressed release of ^{3}H-AA, thus confirming a role for $iPLA_2$ in Ca^{2+}-

independent lipid release **(Figure 1F)**. ^{3}H-AA release was only observed when agonist-induced increases in cytosolic Ca^{2+} were blocked **(Figures 1D-E)**, suggesting that intracellular Ca^{2+} inhibits the Ca^{2+}-independent $iPLA_2$.

Calmodulin is a potent Ca^{2+}-dependent inhibitor of $iPLA_2$ (Wolf and Gross, 1996). To assess the interaction between calmodulin and $iPLA_2$, the cells were treated with Calmidazolium (CMZ), an inhibitor of Ca^{2+}/calmodulin interaction that has been shown to remove the calmodulin block of $iPLA_2$ (Wolf and Gross, 1996). In the presence of CMZ (2 μM), ATP led to a significant release of ^{3}H-AA, which was comparable to blocking increases in cytosolic Ca^{2+} by preloading astrocytes with either CPA or BAPTA **(Figure 1E)**. This observation suggests that Ca^{2+} acts primarily as a brake, through calmodulin, that effectively inhibits $iPLA_2$ activity (Wolf and Gross, 1996; Wolf et al., 1997). These findings are consistent with previous studies showing that $iPLA_2$ is involved in receptor-mediated AA release in pancreatic islet cells (Gross et al., 1993), smooth muscle cells (Lehman et al., 1993), and endothelial cells (Seegers et al., 2002). Taken together, these data provide evidence of a new signaling mechanism in astrocytes through Ca^{2+}-independent $iPLA_2$, which is the major PLA_2 isoform in the brain and accounting for 70% of total PLA_2 activity (Yang et al., 1999).

Targeted lipidomics reveals multiple lipid species produced in cultured astrocytes through Ca^{2+} independent mechanisms

Using lipid extraction and partial purification methods coupled to HPLC/MS/MS, targeted lipidomics screens were performed on cultured astrocytes that were incubated with CPA and then challenged with ATP and compared to vehicle controls. Of the 50 lipids that were screened, 30 were present in each of the samples and could be used for comparative analyses. Table 1 lists all of the actual values as mean ±SEM **(Figure 2A)**. **Figure 2A** summarizes those with significant differences as well as the magnitude of the differences. Of the 30 lipids detected, 16 increased with ATP in the presence of CPA including AA and PGE_2. **Figures 2B-C** are representative chromatograms of the HPLC/MS/MS methods used for detection of PGE_2. Notably, 5 of the 8 AA-

derivatives were significantly increased, including the endocannabinoids, anandamide and 2-AG, though the most dramatic increases were of the prostaglandin, PGE_2. **Figure 2D** shows representative differences in three of the AA-derivatives screened.

GPCR-mediated Ca^{2+} independent release of PGE_2 from astrocytic cultures

Given that Ca^{2+}-dependent astrocyte lipid release has been previously implicated in vasoregulation (Zonta et al., 2003; Takano et al., 2006; Gordon et al., 2008), it was surprising that PGE_2 was released via a Ca^{2+}-independent mechanism. Since HPCL/MS/MS methods required large quantities of cells to detect PGE_2, whereas the PGE_2 ELISA assay accurately detects PGE_2 release in 24-well cultures, we used ELISA to explore and define the Ca^{2+} dependence of astrocytic PGE_2 release. Because $iPLA_2$ is essential for Ca^{2+} independent liberation of AA derived lipids, we first assessed whether knockdown of $iPLA_2$ via viral transduction would inhibit astrocytic release of PGE_2. In the presence of CPA (20 μM), ATP (100 μM) failed to induce PGE_2 release in astrocytic cultures viral transduced with shRNA, whereas a significant increase in the release of PGE_2 was observed in the presence of ATP and CPA in control shRNA cultures **(Figure 3A)**. Knockdown of $iPLA_2$ via shRNA viral transduction was confirmed with western blot analysis **(Figure 3B)**.

Since cultured astrocytes express mGluR5 (Balazs et al., 1997; Silva et al., 1999; Gebremedhin et al., 2003), we next tested whether tACPD (100 μM) and AMPA (100 μM) in the presence and absence of CPA evoked PGE_2 release. In the absence of CPA, little to no release of PGE_2 was observed **(Figure 3C)**. However, when CPA blocked release of Ca^{2+} from internal stores , tACPD and AMPA significantly increased PGE_2 release **(Figure 3C)**.

The most abundant mGluR receptors expressed by astrocytes are mGluR5 and mGluR3 (Petralia et al., 1996; Aronica et al., 2000; Tamaru et al., 2001). However, mGluR5 is developmentally regulated and is not expressed by astrocytes in the adult brain, whereas mGluR3 is persistently expressed at high levels throughout adulthood (Sun et al., 2013). It is therefore important to know whether activation of mGluR3 can induce Ca^{2+}-independent PGE_2 release

since activation of this receptor has recently been shown to induce Ca^{2+} transients in adult hippocampal astrocytes (Haustein et al., 2014; Tang et al., 2015). In the presence of CPA, mGluR3 agonists, NAAG and LY379268, (Wroblewska et al., 1997; Bond et al., 1999) evoked a significant increase in the release of PGE_2, whereas the same agonists failed to release PGE_2 in the absence of CPA **(Figure 3D)**. This is interesting because it shows that activation of an astrocytic Gi-coupled receptor can release gliotransmitters in a Ca^{2+}-independent mechanism.

To extend the observation to human astrocytes, we performed the same experiments in primary cultured astrocytes harvested from embryonic tissue (Windrem et al., 2004; Windrem et al., 2008; Han et al., 2013). After pharmacologically assessing $iPLA_2$ activity in rat astrocytes **(Figure 1F)**, we evaluated $iPLA_2$ expression in all the culture models. Western blot analysis showed that $iPLA_2$ expression was not limited to rat astrocytic cultures, but was also readily expressed in both human and mouse astrocytes **(Figure 3E)**. In the presence of CPA, ATP evoked a significant PGE_2 release from cultured human astrocytes, whereas little to no release was observed with ATP alone **(Figure 3F)**. Likewise, co-application of tACPD and AMPA showed the same effect **(Figure 3F)**. Taken together, these findings show that ATP or mGluR3 activation lead to Ca^{2+}-independent PGE_2 release and that $iPLA_2$ is expressed in mouse, rat, and human astrocytic cultures.

Ca^{2+}-independent astrocytic lipid release enhances mEPSPs via Kv channel blockade

Experiments thus far have demonstrated that cultured astrocytes in response to agonist exposure can indeed release lipids in a Ca^{2+}-independent pathway. In fact, the in vitro analysis showed that agonist-induced Ca^{2+} increases impede PGE_2 release as CPA, BAPTA, and CMZ pretreatment potentiated PGE_2 release.

Earlier studies have shown that AA and its metabolite, PGE_2, inhibit neuronal Kv current (Horimoto et al., 1997; Nicol et al., 1997; Evans et al., 1999) and thereby enhance excitability (Sekiyama et al., 1995; Chen and Bazan, 2005; Sang et al., 2005). We next evaluated whether

astrocytic lipid release also inhibits neuronal Kv current and enhances excitability in acute hippocampal slices. We performed dual patch-clamp recordings of pairs of CA1 pyramidal neurons and astrocytes in acute hippocampal brain slices prepared from 12-18 day old mice **(Figure 4A)**. In order to isolate transiently active potassium currents, we used voltage ramps within approximately 100ms, which is fast enough to capture transient A-type currents (Phillips et al., 2018). It is worth noting that the I-V ramp is a good way to discern what voltage deflection in outward current the drugs might affect (Jackson and Bean, 2007). We recorded Kv currents in CA1 neurons as an assay for astrocytic lipid release, since Kv currents are sensitive to AA and/or its metabolites (Villarroel and Schwarz, 1996; Carta et al., 2014). Kv currents were isolated by adding 1 mM QX314 in the patch pipette to block sodium channels (Talbot and Sayer, 1996; Kim et al., 2010) and imposing a voltage ramp (from -100 mV to 50 mV) every 5 seconds to continuously monitor changes in Kv channel current (Ji et al., 2000; Rangroo Thrane et al., 2013b; Carta et al., 2014) as an assay for agonist-induced astrocytic lipid release (Figure 4A). As expected, direct puffing of PGE_2 (50 μM) and AA (50 μM) with a micropipette induced changes in Kv current. The Kv current was significantly reduced in the presence of both PGE2 (50 μM) and AA (50 μM), which is consistent with previous studies (Evans et al., 1999; Carta et al., 2014) **(Figure 4B-C)**.

Is astrocytic release of AA and its metabolites sufficient to increase CA1 neuronal excitability? To assess the effects of astrocytic Ca^{2+} signaling on neighboring neuronal Kv channels, we first stimulated astrocytes with ATP and TFLLR-NH_2, an agonist of protease-activated receptor-1 (PAR1) that is primarily expressed by astrocytes (Shigetomi et al., 2008). ATP (100 μM) induced a comparable change to neuronal Kv when BAPTA (50 μM) was present in the astrocyte patch pipette, but not when it was absent **(Figure 4B-C).** A similar transient decrease in Kv current was observed when astrocytes were activated by TFLLR-NH_2 (30μM). Again, the reduction in neuronal Kv currents was only detected when TFLLR was applied and BAPTA was added to the astrocytic pipette solution **(Fig. 4B-C).** To selectively activate astrocytic

Ca^{2+} signaling, we next employed MrgA1 transgenic animals ($MrgA1^{+/-}$), which express the exogenous Gq-coupled MRG receptor (MrgA1) under control of the GFAP promoter. The MrgA1 agonist, Phe-Met-Arg-Phe amide (FMRF), mobilizes intracellular astrocytic Ca^{2+} stores, enabling assessment of the effects of astrocytic Ca^{2+} signaling on neighboring neuronal Kv currents. Although FMRF (15 μM), induces potent and selective increases in astrocytic cytosolic Ca^{2+} in hippocampal slices (Fiacco et al., 2007; Agulhon et al., 2010; Wang et al., 2012), no detectable changes in neuronal Kv current were detected when the pipette used to patch the astrocyte did not contain BAPTA **(Figure 4B-C)**. However, when BAPTA was included in the astrocyte patch pipette, a marked decrease in neuronal Kv current was evoked by FMRF exposure **(Figure 4B-C)**. Thus, these observations suggest that astrocytes can modulate neuronal Kv current via previously undocumented Ca^{2+}-independent lipid release.

To assess whether a decrease in neuronal Kv current is a consequence of Ca^{2+}-independent astrocytic lipid release, we next employed specific lipid receptor antagonists for PGE_2 and endocannabinoids. Since PGE_2 receptors 1, 2, 3, and 4 are expressed on hippocampal pyramidal neurons (Andreasson, 2010; Maingret et al., 2017), we employed AH6809, a PGE_2 EP1,2, and 3 antagonist (Abramovitz et al., 2000; Ganesh, 2014), and GW627368, a PGE_2 EP4 antagonist (Jones and Chan, 2005; Wilson et al., 2006). In the presence of AH6809 (10 μM) and GW627368X (3 μM) in the perfusion solution, the TFLLR, FMRF, and ATP Ca^{2+}-independent PGE_2 induced decrease in neuronal Kv current was abolished **(Figure 4C)**; In contrast, AM251 (5 μM), a CB1 antagonist, failed to abolish the decrease in Kv current **(Figure 4C)**. Taken together, these data suggest that the observed decrease in neuronal Kv current is a result of astrocytic Ca^{2+}-independent release of PGE_2.

Interestingly, the presence or absence of BAPTA in the astrocytic pipette solution also affected agonist-induced changes in neuronal membrane potential **(Figure 4D)**. Without BAPTA in astrocytes, TFLLR induced hyperpolarization (-2.4 ± 0.26 mV) **(Figure 4D)**, which has been

linked to a decrease in extracellular potassium (Wang et al., 2012). However, with BAPTA present in astrocytes, TFLLR induced depolarization (2.1 ± 0.25 mV) **(Figure 4D)**, an effect we suggest might be attributable to the blockage of potassium current.

PGE_2 has previously been shown to enhance neuronal mEPSPs (Sekiyama et al., 1995) (Sang et al., 2005). We here found that TFLLR-induced activation of astrocytes in slices triggered a decrease in mEPSP amplitude and frequency in the normal hippocampal slices **(Figure 5A)**. The opposite effect, an increase in the amplitude and frequency of mEPSPs was observable only when BAPTA was added to the astrocytic pipette solution **(Figure 5B)**. This observation supports the notion that astrocytic Ca^{2+}-independent lipid release may function as a signaling mechanism capable of modulating synaptic activity by blocking Kv channels, which in turn may increase the frequency and amplitude of mEPSPs. It is interesting that TFLLR's opposing effects on mEPSP amplitude and frequency are dependent upon astrocytic Ca^{2+} levels (**Figure 5C-D**); suggesting Ca^{2+} deletion provides a pathway to PGE_2 enhancement of neuronal excitability.

DISCUSSION

Lipidomics has the potential to open exciting new avenues within the field of gliotransmission. In the present study, we utilized a series of lipidomics methodologies which showed that Ca^{2+} chelation followed by glutamatergic or purinergic receptor stimulation produces a variety of lipids in astrocytes and drives the release of astrocytic PGE_2, which serves to modulate neuronal Kv channels resulting in enhanced synaptic activity detected as an increase in mEPSP amplitude and frequency **(Figure 5)**. Multiple lines of evidence presented here also support the hypothesis that this agonist-induced Ca^{2+}-independent lipid release in astrocytes is $iPLA_2$ dependent. In addition, we demonstrated that receptor mediated Ca^{2+}-independent PGE_2 release was preserved across rat and human astrocytes **(Figure 3)**. The observations reported here represent, to our knowledge, the first demonstration of Ca^{2+}-independent release of

gliotransmitters in the form of lipid mediators and adds a novel dimension to our understanding of glial-neuronal communication.

Importance of $iPLA_2$ pathway in Ca^{2+}-independent astrocytic lipid production

To date, many studies have shown the multifaceted functions of PLA_2 in the CNS, but $iPLA_2$ is the major PLA_2 isoform, and accounts for 70% of the PLA_2 activity in the rat brain (Yang et al., 1999). Although the effects of $cPLA_2$ activation is best documented (Malaplate-Armand et al., 2006; Schaeffer and Gattaz, 2007; Kim et al., 2008), $iPLA_2$ has also been shown to participate in phospholipid remodeling (Sun et al., 2004), regulate hippocampal AMPA receptors and learning and memory (Menard et al., 2005), regulate store-operated Ca^{2+} entry in cerebellar astrocytes (Singaravelu et al., 2006), and provide neuroprotection against oxygen glucose deprivation (Strokin et al., 2006). Astrocytes express both isoforms of PLA_2 (Sun et al., 2005). Numerous studies have documented that PLA_2 is activated in response to agonist induced Ca^{2+} signaling and mediates release of AA and/or its metabolites from astrocytes (Bruner and Murphy, 1990; Stella et al., 1994; Stella et al., 1997; Chen and Chen, 1998). Here, we focused on the largely unexplored $iPLA_2$ lipid pathway in astrocytes. Given the ubiquitous expression of $iPLA_2$ in astrocytes throughout the brain, the argument can be made that it may have multiple signaling roles. Data presented here provide strong evidence for $iPLA_2$ in agonist-induced Ca^{2+}-independent astrocyte lipid release **(Figure 6)**.

Rapid signaling may be the key to astrocytic release of PGE_2 that modulates neuronal Kv channels

An important aspect of astrocytic gliotransmitter release is timing. Agonist-induced astrocytic Ca^{2+} increases occur on a slow time scale of seconds (Cornell-Bell et al., 1990; Wang et al., 2006; Srinivasan et al., 2015) and Ca^{2+} is a key step in gliotransmitter release, (Parpura et al., 1994; Bezzi et al., 1998; Kang et al., 1998), such as ATP (Coco et al., 2003; Parpura and Zorec, 2010; Illes et al., 2019) and D-Serine (Mothet et al., 2000; Yang et al., 2003; Li et al., 2018;

Neame et al., 2019). Recently, we have shown that agonist-induced astrocytic Ca^{2+} signaling could modulate synaptic activity by active K^+ uptake resulting in a transient lowering of extracellular K^+ and depression of synaptic activity (Wang et al., 2012). More recently, we demonstrated that astrocytes can modulate a rapid form of synaptic activity (≥500ms) via 2AG release upon mGluR3 receptor stimulation (Smith et al., 2019). Because receptor mediated astrocytic Ca^{2+} drives K^+ uptake and release of gliotransmitters, these processes must, therefore, occur over a relatively prolonged time course (>500ms). However, agonist-induced Ca^{2+}-independent $iPLA_2$ lipid release, does not require mobilization of intracellular Ca^{2+} stores and this signaling pathway has the potential to signal on a much faster time scale (possibly 10s of milliseconds). We speculate that $iPLA_2$ mediated lipid release may act as a feedback system that enhances fast synaptic transmission in the immediate short-term or under minimal activity conditions with subsequent activity-mediated Ca^{2+} increases serving as a brake to the calmodulin-dependent inhibition of $iPLA_2$. The slower Ca^{2+}-dependent release of gliotransmitters and K^+ uptake is more suited toward the slow and widespread modulation of brain activity (typically inhibition) that occurs in the setting of, for example, activation of locus coeruleus and associated norepinephrine release (Bekar et al., 2008; Ding et al., 2013).

Voltage-gated potassium channels are located on the dendrites of hippocampal pyramidal neurons (Johnston et al., 2000), and these channels play a major role in controlling dendritic excitability by modulating the amplitude of mEPSPs. A morphological study found that the density of Kv channels in the dendrites of pyramidal neurons increased 5-fold from the soma to the most distal point measured in the apical dendrites (Hoffman et al., 1997). Closure of voltage-gated K^+ currents will enhance EPSPs, possibly explaining why PGE_2 enhances synaptic transmission and LTP (Sang et al., 2005).

Lipidomics models as a guide for future gliotransmitter discoveries

Lipidomics is one of the fastest-growing branches of the metabolomics fields with a potential to identify and characterize thousands of lipid species throughout the body, especially in the brain, where the total dry mass of the structure is made primarily of lipids (Sinclair, 1975). The surface to volume ratio of astrocytes is larger than most other cell types based on complex fine structure of laminate, fine astrocytic processes: It is logical that many gliotransmitters would also be lipids. HPLC/MS/MS lipidomics techniques have provided a means to identify specific lipid species with an accuracy that eluded former techniques; however, many of those previously used techniques such as radio-labeled fatty acids and ELISAs are still powerful tools in the field. Here, we have used a combination of these techniques to critically test the hypothesis that lipids are produced in and released from astrocytes in a Ca^{2+}-independent manner. Our focus here was on the release of PGE_2; however, there were 15 additional lipids identified that were upregulated under the same conditions. It is also important to note, that of the 30 lipids detected in this small, targeted HPLC/MS/MS assay, 14 did not change supporting the specificity of GPCR stimulated, Ca^{2+}-independent lipid production. Interestingly, 2 of the lipids released in response to agonist exposure, *N*-arachidonyl taurine and *N*-palmitoyl tyrosine, were recently shown to activate TRPV4 (Raboune et al., 2014). Emerging evidence suggests a role for a TRPV4/AQP4 complex in regulation of hypo-osmotic stress in astrocytes (Benfenati et al., 2011). The lipidomics data provided here can provide unbiased insight into other signaling mechanisms that involve astrocytic-derived lipid modulators **(Figure 2)**.

In conclusion, Ca^{2+}-independent astrocytic lipid release constitutes a largely unexplored participant in complex neuro-glial signaling interactions. The analysis presented here adds a new dimension to agonist-induced Ca^{2+} signaling by demonstrating that several Gq and Gi-linked receptors can mediate release of lipid modulators and that increases in cytosolic Ca^{2+} acts as a break that prevents PGE_2 release.

Author contributions:

F.W., H.B.B., and N.A.S. performed the experiments. F.W., H.B.B., J.X., and N.A.S. analyzed data. S.P. and B.J. performed Western Blots. S.G. and B.L. made cultures. L.B. and N.A.S. planned the experiments. D.C.M. provided Human Astrocytes. F.W., H.B.B., and N.A.S. wrote the paper.

Acknowledgments:
We thank Dr. Ken McCarthy for generously sharing transgenic mice. This work was supported by National Institutes of Health Grant K01NS110981 and NSF1926781 to N.A.S. We thank Vittorio Gallo, Baljit Khakh, Bartosz Kula, Stefano Vicini, Alexander S. Thrane, Vinita Rangroo Thrane, Takahiro Takano, and Fernando R. Fernandez for comments and critical discussion for this manuscript. The authors declare no competing financial interest.

Figure Legends

Figure 1: GPCR-mediated Ca^{2+} independent release of ^{3}H-AA and/ or its metabolites from astrocytic cultures.

A.) Cultured astrocytes were transduced with AAV GFAP cyto-GCaMP6f and the fluorescent changes associated with intracellular Ca^{2+} increases upon ATP stimulation were measured using confocal microscopy. B.) Representative individual traces of GCaMP6f fluorescence changes ($\Delta F/F_0$) in response to ATP stimulation (upper panel). BAPTA-AM (20 μM, n=5 wells) and CPA (20 μM, n=5 wells) eliminated the ATP (100 μM, n=5 wells) evoked Ca^{2+} increases in fluorescent. MAFP (10μM, n=5 wells), Bel (10μM, n=5 wells) did not inhibit ATP (100 μM) induced Ca^{2+}rises in Astrocytes. ***P≤0.0001, Tukey post-hoc test (lower panel). C.) Schematic of the ^{3}H-AA Radioactive Assay. D.) The effects of ATP (100 μM, n=45 wells), CPA (20 μM, n=9 wells), ATP/CPA (n=44 wells), and ATP/BAPTA-AM (n=24 wells) on Ca^{2+} independent release of ^{3}H-AA and its derivatives in astrocytic cultures compared to control and each other. ***P≤0.0001; **P≤0.001; *P≤0.05, Tukey post-hoc test. E.) The effects of mGluR agonists tACPD/AMPA (100 μM, n=7), tACPD/AMPA/CPA (n=7 wells), and ATP/CPA (n=7 wells) on Ca^{2+}-independent release of ^{3}H-AA and its derivatives in astrocytic cultures compared to control and each other. ***P≤0.0001; **P≤0.001; *P≤0.05, Tukey post-hoc test. F.) Effects of the $iPLA_2$ inhibitor, BEL (10 μM, n=12 wells), $cPLA_2$ inhibitor, MAFP (10 μM, n=12 wells), or Calmodulin/Ca^{2+} complex inhibitor, CMZ (2 μM, n=20 wells) co-applied with ATP on Ca^{2+} independent release of ^{3}H-AA and its derivatives in astrocytic cultures compared to ATP alone. ***P≤0.0001; **P≤0.001, Tukey post-hoc test. All bar graphs show means ± s.e.m.

Figure 2. Targeted lipidomics of rat astrocytic cultures using HPLC/MS/MS.

A.) Summary of the significant differences and the magnitude of change between the vehicle controls and the CPA/ATP stimulated cells for the 30 lipids in the screen that were detected across samples. Dark green denotes those significant differences that were

p≤0.05; light green denotes those significant differences between p≤0.10 and 0.05. No differences are signified by "*n.d.*". Arrows indicate the magnitude of effect as indicated in the legend. *Raw data and statistical analyses for all lipids detected are shown in Table 1.* B.) Example chromatograph of a 1pmol of PGE2 standard as analyzed by the HPLC/MS/MS method optimized for this standard in negative ion mode. C.) Example of an analysis of a partially purified astrocytic extract using the HPLC/MS/MS method that is optimized for PGE2. D.) Differences in astrocytic production of the three AA derivative, PGE2, Anandamide (AEA), and 2-arachidonoyl glycerol (2-AG) expressed as the average of the moles/sample; vehicle n=3 flask, CPA/ATP n=4 flask.

Figure 3: GPCR-mediated Ca^{2+} independent release of PGE_2 from astrocytic cultures.

A.) The effects of ATP (100 μM, n=4 wells) and ATP/CPA (n=4 wells) on Ca^{2+} independent PGE_2 release in rat astrocytic cultures virally transduced with shRNA to knockdown $iPLA_2$ comparted to control shRNA cultures. *P≤0.05, Dunn post-test. B.) Western blot analysis of $iPLA_2$ knockdown via shRNA. β-actin specific antibody was used to standardize for equal protein loading. C.) The effects of GPCR agonists ATP (100 μM, n=12 wells), tACPD/AMPA (100μM, n=7 wells), tACPD/AMPA/CPA (n=7), and ATP/CPA (n=12 wells) on Ca^{2+}-independent PGE_2 release in rat astrocytic cultures compared to control. ****P≤0.0001; ***P≤0.001, Tukey post-test. D.) The effects of ATP/CPA (100uM, n=4) and mGluR3 agonist NAAG (100 μM, n=4 wells), LY379268 (100 μM, n=4 wells), NAAG/CPA (n=4), and LY379268/CPA (n=4 wells) on Ca^{2+}-independent PGE_2 release in rat astrocytic cultures compared to control and each other. ***P≤0.001, Tukey post-test. E.) Western blot analysis of $iPLA_2$ protein for Human, Rat, and Mouse cultures. β-actin specific antibody was used to standardize for equal protein loading. F.) The effects of GPCR agonists ATP (100 μM, n=8 wells), ATP/CPA (n=8 wells), tACPD/AMPA (100 μM, n=8 wells), and tACPD/AMPA/CPA (n=8 wells) on Ca^{2+}-independent PGE_2 release in human astrocytic cultures

compared to control and each other. ***P≤0.0001; **P≤0.001; *P≤0.05, Tukey post-hoc test. All bar graphs show means ± s.e.m.

Figure 4: Ca^{2+}-independent astrocytic lipid release inhibits Kv channel blockade.

Image of a patched astrocyte and a patched neuron, filled with fluorescent dyes. B.) Direct application of AA (50 μM) and PGE2 (50 μM) decreased Kv current. TFLLR (30 μM) and ATP (100 μM), with BAPTA also decreased Kv current, as can be seen in the peak currents. FMRF (15 μM) in the $MrgA1^{+/-}$ mice applied in the presence of BAPTA decreased Kv current, but not in the absence of BAPTA. Traces to the left are representative recordings of changes to membrane voltages in the presence of drugs described above. C.) Quantification of effects of different drugs on the holding voltage ramp induced voltage gated K^+ currents (*, $P < 0.05$, **, $p < 0.01$, n =5-7 mice). D.) Representative traces showing changes to membrane potentials VM upon TFLLR application in the presence or absence of BAPTA, and quantifications are shown in inset (**, $p < 0.01$, t-test, n =5-6 mice). All bar graphs show means ± s.e.m.

Figure 5: Ca^{2+}-independent astrocytic lipid release increase mEPSP amplitude and frequency.

A.) Representative trace showing hyperpolarization and reduction in mEPSP amplitude and frequency in excitatory hippocampal neurons upon TFLLR (30 μM) application without BAPTA being present in neighboring astrocytes. B.) Representative trace showing depolarization and an increase in mEPSP amplitude and frequency in excitatory hippocampal neurons upon TFLLR (30 μM) application with BAPTA present in neighboring astrocytes. Lower traces are extensions of parts of recordings in upper trace. C.) Comparison of the cumulative mEPSP amplitude and cumulative mEPSP frequency distribution recorded in B). D.) Statistical analysis of the amplitude and inter-event intervals before and after TFLLR application, with and without BAPTA present (**, p < 001, paired t-test, N =5-7 mice). All bar graphs show means ± s.e.m.

Figure 6: Models of GPCR-mediated Ca^{2+}-independent and Ca^{2+}-dependent lipid release in astrocytes.

A.) Schematic of receptor mediated Ca^{2+}-Independent lipid release across the astrocytic membrane. B.) Schematic of receptor mediated Ca^{2+}-Dependent lipid release across the astrocytic membrane.

References

Abramovitz M, Adam M, Boie Y, Carriere M, Denis D, Godbout C, Lamontagne S, Rochette C, Sawyer N, Tremblay NM, Belley M, Gallant M, Dufresne C, Gareau Y, Ruel R, Juteau H, Labelle M, Ouimet N, Metters KM (2000) The utilization of recombinant prostanoid receptors to determine the affinities and selectivities of prostaglandins and related analogs. Biochim Biophys Acta 1483:285-293.

Agulhon C, Fiacco TA, McCarthy KD (2010) Hippocampal short- and long-term plasticity are not modulated by astrocyte Ca2+ signaling. Science 327:1250-1254.

Akiba S, Hayama M, Sato T (1998) Inhibition of Ca2+-independent phospholipase A2 by bromoenol lactone attenuates prostaglandin generation induced by interleukin-1 beta and dibutyryl cAMP in rat mesangial cells. FEBS Lett 437:225-228.

Andreasson K (2010) Emerging roles of PGE2 receptors in models of neurological disease. Prostaglandins Other Lipid Mediat 91:104-112.

Aronica E, van Vliet EA, Mayboroda OA, Troost D, da Silva FH, Gorter JA (2000) Upregulation of metabotropic glutamate receptor subtype mGluR3 and mGluR5 in reactive astrocytes in a rat model of mesial temporal lobe epilepsy. The European journal of neuroscience 12:2333-2344.

Balazs R, Miller S, Romano C, de Vries A, Chun Y, Cotman CW (1997) Metabotropic glutamate receptor mGluR5 in astrocytes: pharmacological properties and agonist regulation. J Neurochem 69:151-163.

Bekar LK, He W, Nedergaard M (2008) Locus coeruleus alpha-adrenergic-mediated activation of cortical astrocytes in vivo. Cerebral cortex 18:2789-2795.

Benfenati V, Caprini M, Dovizio M, Mylonakou MN, Ferroni S, Ottersen OP, Amiry-Moghaddam M (2011) An aquaporin-4/transient receptor potential vanilloid 4 (AQP4/TRPV4) complex is essential for cell-volume control in astrocytes. Proc Natl Acad Sci U S A 108:2563-2568.

Bezzi P, Carmignoto G, Pasti L, Vesce S, Rossi D, Rizzini BL, Pozzan T, Volterra A (1998) Prostaglandins stimulate calcium-dependent glutamate release in astrocytes. Nature 391:281-285.

Boland LM, Drzewiecki MM (2008) Polyunsaturated fatty acid modulation of voltage-gated ion channels. Cell biochemistry and biophysics 52:59-84.

Bond A, Ragumoorthy N, Monn JA, Hicks CA, Ward MA, Lodge D, O'Neill MJ (1999) LY379268, a potent and selective Group II metabotropic glutamate receptor agonist, is neuroprotective in gerbil global, but not focal, cerebral ischaemia. Neurosci Lett 273:191-194.

Bruner G, Murphy S (1990) ATP-evoked arachidonic acid mobilization in astrocytes is via a P2Y-purinergic receptor. J Neurochem 55:1569-1575.

Carta M, Lanore F, Rebola N, Szabo Z, Da Silva SV, Lourenco J, Verraes A, Nadler A, Schultz C, Blanchet C, Mulle C (2014) Membrane Lipids Tune Synaptic Transmission by Direct Modulation of Presynaptic Potassium Channels. Neuron.

Chen C, Bazan NG (2005) Endogenous PGE2 regulates membrane excitability and synaptic transmission in hippocampal CA1 pyramidal neurons. J Neurophysiol 93:929-941.

Chen WC, Chen CC (1998) ATP-induced arachidonic acid release in cultured astrocytes is mediated by Gi protein coupled P2Y1 and P2Y2 receptors. Glia 22:360-370.

Coco S, Calegari F, Pravettoni E, Pozzi D, Taverna E, Rosa P, Matteoli M, Verderio C (2003) Storage and release of ATP from astrocytes in culture. J Biol Chem 278:1354-1362.

Cordero-Morales JF, Vasquez V (2018) How lipids contribute to ion channel function, a fat perspective on direct and indirect interactions. Curr Opin Struct Biol 51:92-98.

Cornell-Bell AH, Finkbeiner SM, Cooper MS, Smith SJ (1990) Glutamate induces calcium waves in cultured astrocytes: long-range glial signaling. Science 247:470-473.

Czigler A, Toth L, Szarka N, Szilagyi K, Kellermayer Z, Harci A, Vecsernyes M, Ungvari Z, Szolics A, Koller A, Buki A, Toth P (2019) Prostaglandin E2, a postulated mediator of neurovascular coupling, at low concentrations dilates whereas at higher concentrations constricts human cerebral parenchymal arterioles. Prostaglandins Other Lipid Mediat 146:106389.

Dabertrand F, Hannah RM, Pearson JM, Hill-Eubanks DC, Brayden JE, Nelson MT (2013) Prostaglandin E2, a postulated astrocyte-derived neurovascular coupling agent, constricts rather than dilates parenchymal arterioles. J Cereb Blood Flow Metab 33:479-482.

Dhopeshwarkar GA, Subramanian C (1976) Biosynthesis of polyunsaturated fatty acids in the developing brain: I. Metabolic transformations of intracranially administered 1-14C linolenic acid. Lipids 11:67-71.

Ding F, O'Donnell J, Thrane AS, Zeppenfeld D, Kang H, Xie L, Wang F, Nedergaard M (2013) alpha1-Adrenergic receptors mediate coordinated Ca2+ signaling of cortical astrocytes in awake, behaving mice. Cell calcium 54:387-394.

Evans AR, Vasko MR, Nicol GD (1999) The cAMP transduction cascade mediates the PGE2-induced inhibition of potassium currents in rat sensory neurones. J Physiol 516 (Pt 1):163-178.

Fiacco TA, Agulhon C, Taves SR, Petravicz J, Casper KB, Dong X, Chen J, McCarthy KD (2007) Selective stimulation of astrocyte calcium in situ does not affect neuronal excitatory synaptic activity. Neuron 54:611-626.

Fride E (2002) Endocannabinoids in the central nervous system--an overview. Prostaglandins, leukotrienes, and essential fatty acids 66:221-233.

Ganesh T (2014) Prostanoid receptor EP2 as a therapeutic target. J Med Chem 57:4454-4465.

Gebremedhin D, Yamaura K, Zhang C, Bylund J, Koehler RC, Harder DR (2003) Metabotropic glutamate receptor activation enhances the activities of two types of Ca2+-activated k+ channels in rat hippocampal astrocytes. The Journal of neuroscience : the official journal of the Society for Neuroscience 23:1678-1687.

Gordon GR, Mulligan SJ, MacVicar BA (2007) Astrocyte control of the cerebrovasculature. Glia 55:1214-1221.

Gordon GR, Choi HB, Rungta RL, Ellis-Davies GC, MacVicar BA (2008) Brain metabolism dictates the polarity of astrocyte control over arterioles. Nature 456:745-749.

Gross RW, Ramanadham S, Kruszka KK, Han X, Turk J (1993) Rat and human pancreatic islet cells contain a calcium ion independent phospholipase A2 activity selective for hydrolysis of arachidonate which is stimulated by adenosine triphosphate and is specifically localized to islet beta-cells. Biochemistry 32:327-336.

Han X, Chen M, Wang F, Windrem M, Wang S, Shanz S, Xu Q, Oberheim NA, Bekar L, Betstadt S, Silva AJ, Takano T, Goldman SA, Nedergaard M (2013) Forebrain engraftment by human glial progenitor cells enhances synaptic plasticity and learning in adult mice. Cell Stem Cell 12:342-353.

Hashimotodani Y, Ohno-Shosaku T, Kano M (2007) Endocannabinoids and synaptic function in the CNS. Neuroscientist 13:127-137.

Haustein MD, Kracun S, Lu XH, Shih T, Jackson-Weaver O, Tong X, Xu J, Yang XW, O'Dell TJ, Marvin JS, Ellisman MH, Bushong EA, Looger LL, Khakh BS (2014) Conditions and constraints for astrocyte calcium signaling in the hippocampal mossy fiber pathway. Neuron 82:413-429.

Hoffman DA, Magee JC, Colbert CM, Johnston D (1997) K+ channel regulation of signal propagation in dendrites of hippocampal pyramidal neurons. Nature 387:869-875.

Horimoto N, Nabekura J, Ogawa T (1997) Arachidonic acid activation of potassium channels in rat visual cortex neurons. Neuroscience 77:661-671.

Illes P, Burnstock G, Tang Y (2019) Astroglia-Derived ATP Modulates CNS Neuronal Circuits. Trends in neurosciences 42:885-898.

Jackson AC, Bean BP (2007) State-dependent enhancement of subthreshold A-type potassium current by 4-aminopyridine in tuberomammillary nucleus neurons. The Journal of neuroscience : the official journal of the Society for Neuroscience 27:10785-10796.

Jelsema CL, Axelrod J (1987) Stimulation of phospholipase A2 activity in bovine rod outer segments by the beta gamma subunits of transducin and its inhibition by the alpha subunit. Proc Natl Acad Sci U S A 84:3623-3627.

Ji J, Salapatek AM, Diamant NE (2000) Inwardly rectifying K(+) channels in esophageal smooth muscle. Am J Physiol Gastrointest Liver Physiol 279:G951-960.

Johnston D, Hoffman DA, Magee JC, Poolos NP, Watanabe S, Colbert CM, Migliore M (2000) Dendritic potassium channels in hippocampal pyramidal neurons. J Physiol 525 Pt 1:75-81.

Jones RL, Chan KM (2005) Investigation of the agonist activity of prostacyclin analogues on prostanoid EP4 receptors using GW 627368 and taprostene: evidence for species differences. Prostaglandins Leukot Essent Fatty Acids 72:289-299.

Kang J, Jiang L, Goldman SA, Nedergaard M (1998) Astrocyte-mediated potentiation of inhibitory synaptic transmission. Nature neuroscience 1:683-692.

Kim DH, Fitzsimmons B, Hefferan MP, Svensson CI, Wancewicz E, Monia BP, Hung G, Butler M, Marsala M, Hua XY, Yaksh TL (2008) Inhibition of spinal cytosolic phospholipase A(2) expression by an antisense oligonucleotide attenuates tissue injury-induced hyperalgesia. Neuroscience 154:1077-1087.

Kim JH, Kushmerick C, von Gersdorff H (2010) Presynaptic resurgent Na+ currents sculpt the action potential waveform and increase firing reliability at a CNS nerve terminal. The Journal of neuroscience : the official journal of the Society for Neuroscience 30:15479-15490.

Ledo A, Rocha BS, Laranjinha J (2019) Bioactive Lipids and the Gut-Brain Axis: Diet as a Modulator of Bioactivity and Diversity of Lipids in the Brain. Adv Exp Med Biol 1127:147-168.

Lehman JJ, Brown KA, Ramanadham S, Turk J, Gross RW (1993) Arachidonic acid release from aortic smooth muscle cells induced by [Arg8]vasopressin is largely mediated by calcium-independent phospholipase A2. J Biol Chem 268:20713-20716.

Leishman E, Manchanda M, Thelen R, Miller S, Mackie K, Bradshaw HB (2018) Cannabidiol's Upregulation of N-acyl Ethanolamines in the Central Nervous System Requires N-acyl Phosphatidyl Ethanolamine-Specific Phospholipase D. Cannabis Cannabinoid Res 3:228-241.

Li S, Uno Y, Rudolph U, Cobb J, Liu J, Anderson T, Levy D, Balu DT, Coyle JT (2018) Astrocytes in primary cultures express serine racemase, synthesize d-serine and acquire A1 reactive astrocyte features. Biochem Pharmacol 151:245-251.

Lin JH, Weigel H, Cotrina ML, Liu S, Bueno E, Hansen AJ, Hansen TW, Goldman S, Nedergaard M (1998) Gap-junction-mediated propagation and amplification of cell injury. Nat Neurosci 1:494-500.

MacVicar BA, Newman EA (2015) Astrocyte regulation of blood flow in the brain. Cold Spring Harb Perspect Biol 7.

Maingret V, Barthet G, Deforges S, Jiang N, Mulle C, Amedee T (2017) PGE2-EP3 signaling pathway impairs hippocampal presynaptic long-term plasticity in a mouse model of Alzheimer's disease. Neurobiol Aging 50:13-24.

Malaplate-Armand C, Florent-Bechard S, Youssef I, Koziel V, Sponne I, Kriem B, Leininger-Muller B, Olivier JL, Oster T, Pillot T (2006) Soluble oligomers of amyloid-beta peptide induce neuronal apoptosis by activating a cPLA2-dependent sphingomyelinase-ceramide pathway. Neurobiol Dis 23:178-189.

Menard C, Valastro B, Martel MA, Chartier E, Marineau A, Baudry M, Massicotte G (2005) AMPA receptor phosphorylation is selectively regulated by constitutive phospholipase A(2) and 5-lipoxygenase activities. Hippocampus 15:370-380.

Meves H (1994) Modulation of ion channels by arachidonic acid. Prog Neurobiol 43:175-186.

Moore SA (1993) Cerebral endothelium and astrocytes cooperate in supplying docosahexaenoic acid to neurons. Adv Exp Med Biol 331:229-233.

Moore SA, Yoder E, Murphy S, Dutton GR, Spector AA (1991) Astrocytes, not neurons, produce docosahexaenoic acid (22:6 omega-3) and arachidonic acid (20:4 omega-6). J Neurochem 56:518-524.

Mothet J, Parent A, Wolosker H, Jr RB, Linden D, Ferris C, Rogawski M, Synder S (2000) D-serine is an endogenous ligand for the site of N-methyl D-aspartate receptor. Proc Natl Acad Sci U S A 97:4926-4931.

Murayama T, Kajiyama Y, Nomura Y (1990) Histamine-stimulated and GTP-binding proteins-mediated phospholipase A2 activation in rabbit platelets. J Biol Chem 265:4290-4295.

Neame S, Safory H, Radzishevsky I, Touitou A, Marchesani F, Marchetti M, Kellner S, Berlin S, Foltyn VN, Engelender S, Billard JM, Wolosker H (2019) The NMDA receptor activation by d-serine and glycine is controlled by an astrocytic Phgdh-dependent serine shuttle. Proceedings of the National Academy of Sciences of the United States of America 116:20736-20742.

Nedergaard M (1994) Direct signaling from astrocytes to neurons in cultures of mammalian brain cells. Science 263:1768-1771.

Nicol GD, Vasko MR, Evans AR (1997) Prostaglandins suppress an outward potassium current in embryonic rat sensory neurons. J Neurophysiol 77:167-176.
Parpura V, Zorec R (2010) Gliotransmission: Exocytotic release from astrocytes. Brain Res Rev 63:83-92.
Parpura V, Basarsky TA, Liu F, Jeftinija K, Jeftinija S, Haydon PG (1994) Glutamate-mediated astrocyte-neuron signalling. Nature 369:744-747.
Petralia RS, Wang YX, Niedzielski AS, Wenthold RJ (1996) The metabotropic glutamate receptors, mGluR2 and mGluR3, show unique postsynaptic, presynaptic and glial localizations. Neuroscience 71:949-976.
Phillips WS, Del Negro CA, Rekling JC (2018) Dendritic A-Current in Rhythmically Active PreBotzinger Complex Neurons in Organotypic Cultures from Newborn Mice. The Journal of neuroscience : the official journal of the Society for Neuroscience 38:3039-3049.
Piomelli D (1993) Arachidonic acid in cell signaling. Current opinion in cell biology 5:274-280.
Plog BA, Nedergaard M (2018) The Glymphatic System in Central Nervous System Health and Disease: Past, Present, and Future. Annu Rev Pathol 13:379-394.
Portilla D, Shah SV, Lehman PA, Creer MH (1994) Role of cytosolic calcium-independent plasmalogen-selective phospholipase A2 in hypoxic injury to rabbit proximal tubules. The Journal of clinical investigation 93:1609-1615.
Ramakers GM, Storm JF (2002) A postsynaptic transient K(+) current modulated by arachidonic acid regulates synaptic integration and threshold for LTP induction in hippocampal pyramidal cells. Proc Natl Acad Sci U S A 99:10144-10149.
Rangroo Thrane V, Thrane AS, Plog BA, Thiyagarajan M, Iliff JJ, Deane R, Nagelhus EA, Nedergaard M (2013a) Paravascular microcirculation facilitates rapid lipid transport and astrocyte signaling in the brain. Sci Rep 3:2582.
Rangroo Thrane V, Thrane AS, Wang F, Cotrina ML, Smith NA, Chen M, Xu Q, Kang N, Fujita T, Nagelhus EA, Nedergaard M (2013b) Ammonia triggers neuronal disinhibition and seizures by impairing astrocyte potassium buffering. Nat Med 19:1643-1648.
Rosenegger DG, Tran CH, Wamsteeker Cusulin JI, Gordon GR (2015) Tonic Local Brain Blood Flow Control by Astrocytes Independent of Phasic Neurovascular Coupling. The Journal of neuroscience : the official journal of the Society for Neuroscience 35:13463-13474.
Sang N, Zhang J, Marcheselli V, Bazan NG, Chen C (2005) Postsynaptically synthesized prostaglandin E2 (PGE2) modulates hippocampal synaptic transmission via a presynaptic PGE2 EP2 receptor. J Neurosci 25:9858-9870.
Schaeffer EL, Gattaz WF (2007) Requirement of hippocampal phospholipase A2 activity for long-term memory retrieval in rats. J Neural Transm 114:379-385.
Seegers HC, Gross RW, Boyle WA (2002) Calcium-independent phospholipase A(2)-derived arachidonic acid is essential for endothelium-dependent relaxation by acetylcholine. J Pharmacol Exp Ther 302:918-923.
Sekiyama N, Mizuta S, Hori A, Kobayashi S (1995) Prostaglandin E2 facilitates excitatory synaptic transmission in the nucleus tractus solitarii of rats. Neurosci Lett 188:101-104.
Shigetomi E, Bowser DN, Sofroniew MV, Khakh BS (2008) Two forms of astrocyte calcium excitability have distinct effects on NMDA receptor-mediated slow inward currents in pyramidal neurons. J Neurosci 28:6659-6663.
Silva GA, Theriault E, Mills LR, Pennefather PS, Feeney CJ (1999) Group I and II metabotropic glutamate receptor expression in cultured rat spinal cord astrocytes. Neurosci Lett 263:117-120.

Sinclair AJ (1975) Long-chain polyunsaturated fatty acids in the mammalian brain. The Proceedings of the Nutrition Society 34:287-291.
Singaravelu K, Lohr C, Deitmer JW (2006) Regulation of store-operated calcium entry by calcium-independent phospholipase A2 in rat cerebellar astrocytes. J Neurosci 26:9579-9592.
Smith NA, Bekar LK, Nedergaard M (2019) Astrocytic Endocannabinoids Mediate Hippocampal Transient Heterosynaptic Depression. Neurochem Res.
Smith NA, Kress BT, Lu Y, Chandler-Militello D, Benraiss A, Nedergaard M (2018) Fluorescent Ca(2+) indicators directly inhibit the Na,K-ATPase and disrupt cellular functions. Sci Signal 11.
Srinivasan R, Huang BS, Venugopal S, Johnston AD, Chai H, Zeng H, Golshani P, Khakh BS (2015) Ca(2+) signaling in astrocytes from Ip3r2(-/-) mice in brain slices and during startle responses in vivo. Nat Neurosci 18:708-717.
Stella N, Tence M, Glowinski J, Premont J (1994) Glutamate-evoked release of arachidonic acid from mouse brain astrocytes. J Neurosci 14:568-575.
Stella N, Estelles A, Siciliano J, Tence M, Desagher S, Piomelli D, Glowinski J, Premont J (1997) Interleukin-1 enhances the ATP-evoked release of arachidonic acid from mouse astrocytes. J Neurosci 17:2939-2946.
Strokin M, Sergeeva M, Reiser G (2003) Docosahexaenoic acid and arachidonic acid release in rat brain astrocytes is mediated by two separate isoforms of phospholipase A2 and is differently regulated by cyclic AMP and Ca2+. Br J Pharmacol 139:1014-1022.
Strokin M, Chechneva O, Reymann KG, Reiser G (2006) Neuroprotection of rat hippocampal slices exposed to oxygen-glucose deprivation by enrichment with docosahexaenoic acid and by inhibition of hydrolysis of docosahexaenoic acid-containing phospholipids by calcium independent phospholipase A2. Neuroscience 140:547-553.
Sun GY, Xu J, Jensen MD, Simonyi A (2004) Phospholipase A2 in the central nervous system: implications for neurodegenerative diseases. Journal of lipid research 45:205-213.
Sun GY, Xu J, Jensen MD, Yu S, Wood WG, Gonzalez FA, Simonyi A, Sun AY, Weisman GA (2005) Phospholipase A2 in astrocytes: responses to oxidative stress, inflammation, and G protein-coupled receptor agonists. Mol Neurobiol 31:27-41.
Sun W, McConnell E, Pare JF, Xu Q, Chen M, Peng W, Lovatt D, Han X, Smith Y, Nedergaard M (2013) Glutamate-dependent neuroglial calcium signaling differs between young and adult brain. Science 339:197-200.
Takano T, Tian GF, Peng W, Lou N, Libionka W, Han X, Nedergaard M (2006) Astrocyte-mediated control of cerebral blood flow. Nat Neurosci 9:260-267.
Talbot MJ, Sayer RJ (1996) Intracellular QX-314 inhibits calcium currents in hippocampal CA1 pyramidal neurons. Journal of neurophysiology 76:2120-2124.
Tamaru Y, Nomura S, Mizuno N, Shigemoto R (2001) Distribution of metabotropic glutamate receptor mGluR3 in the mouse CNS: differential location relative to pre- and postsynaptic sites. Neuroscience 106:481-503.
Tang W, Szokol K, Jensen V, Enger R, Trivedi CA, Hvalby O, Helm PJ, Looger LL, Sprengel R, Nagelhus EA (2015) Stimulation-evoked Ca2+ signals in astrocytic processes at hippocampal CA3-CA1 synapses of adult mice are modulated by glutamate and ATP. The Journal of neuroscience : the official journal of the Society for Neuroscience 35:3016-3021.
Tay HK, Melendez AJ (2004) Fcgamma RI-triggered generation of arachidonic acid and eicosanoids requires iPLA2 but not cPLA2 in human monocytic cells. J Biol Chem 279:22505-22513.

van Tol-Steye H, Lodder JC, Mansvelder HD, Planta RJ, van Heerikhuizen H, Kits KS (1999) Roles of G-protein beta gamma, arachidonic acid, and phosphorylation inconvergent activation of an S-like potassium conductance by dopamine, Ala-Pro-Gly-Trp-NH2, and Phe-Met-Arg-Phe-NH2. J Neurosci 19:3739-3751.

Villarroel A, Schwarz TL (1996) Inhibition of the Kv4 (Shal) family of transient K+ currents by arachidonic acid. The Journal of neuroscience : the official journal of the Society for Neuroscience 16:2522-2532.

Wang F, Smith NA, Xu Q, Fujita T, Baba A, Matsuda T, Takano T, Bekar L, Nedergaard M (2012) Astrocytes modulate neural network activity by Ca(2)+-dependent uptake of extracellular K+. Sci Signal 5:ra26.

Wang X, Lou N, Xu Q, Tian GF, Peng WG, Han X, Kang J, Takano T, Nedergaard M (2006) Astrocytic Ca2+ signaling evoked by sensory stimulation in vivo. Nature neuroscience 9:816-823.

Wilson RJ, Giblin GM, Roomans S, Rhodes SA, Cartwright KA, Shield VJ, Brown J, Wise A, Chowdhury J, Pritchard S, Coote J, Noel LS, Kenakin T, Burns-Kurtis CL, Morrison V, Gray DW, Giles H (2006) GW627368X ((N-{2-[4-(4,9-diethoxy-1-oxo-1,3-dihydro-2H-benzo[f]isoindol-2-yl)phenyl]acetyl} benzene sulphonamide): a novel, potent and selective prostanoid EP4 receptor antagonist. Br J Pharmacol 148:326-339.

Windrem MS, Nunes MC, Rashbaum WK, Schwartz TH, Goodman RA, McKhann G, 2nd, Roy NS, Goldman SA (2004) Fetal and adult human oligodendrocyte progenitor cell isolates myelinate the congenitally dysmyelinated brain. Nat Med 10:93-97.

Windrem MS, Schanz SJ, Guo M, Tian GF, Washco V, Stanwood N, Rasband M, Roy NS, Nedergaard M, Havton LA, Wang S, Goldman SA (2008) Neonatal chimerization with human glial progenitor cells can both remyelinate and rescue the otherwise lethally hypomyelinated shiverer mouse. Cell stem cell 2:553-565.

Winstead MV, Balsinde J, Dennis EA (2000) Calcium-independent phospholipase A(2): structure and function. Biochimica et biophysica acta 1488:28-39.

Wolf MJ, Gross RW (1996) The calcium-dependent association and functional coupling of calmodulin with myocardial phospholipase A2. Implications for cardiac cycle-dependent alterations in phospholipolysis. J Biol Chem 271:20989-20992.

Wolf MJ, Wang J, Turk J, Gross RW (1997) Depletion of intracellular calcium stores activates smooth muscle cell calcium-independent phospholipase A2. A novel mechanism underlying arachidonic acid mobilization. J Biol Chem 272:1522-1526.

Wroblewska B, Wroblewski JT, Pshenichkin S, Surin A, Sullivan SE, Neale JH (1997) N-acetylaspartylglutamate selectively activates mGluR3 receptors in transfected cells. J Neurochem 69:174-181.

Yang HC, Mosior M, Ni B, Dennis EA (1999) Regional distribution, ontogeny, purification, and characterization of the Ca2+-independent phospholipase A2 from rat brain. J Neurochem 73:1278-1287.

Yang Y, Ge W, Chen Y, Zhang Z, Shen W, Wu C, Poo M, Duan S (2003) Contribution of astrocytes to hippocampal long-term potentiation through release of D-serine. Proc Natl Acad Sci U S A 100:15194-15199.

Yu X, Taylor AMW, Nagai J, Golshani P, Evans CJ, Coppola G, Khakh BS (2018) Reducing Astrocyte Calcium Signaling In Vivo Alters Striatal Microcircuits and Causes Repetitive Behavior. Neuron 99:1170-1187 e1179.

Zonta M, Angulo MC, Gobbo S, Rosengarten B, Hossmann KA, Pozzan T, Carmignoto G (2003) Neuron-to-astrocyte signaling is central to the dynamic control of brain microcirculation. Nat Neurosci 6:43-50.

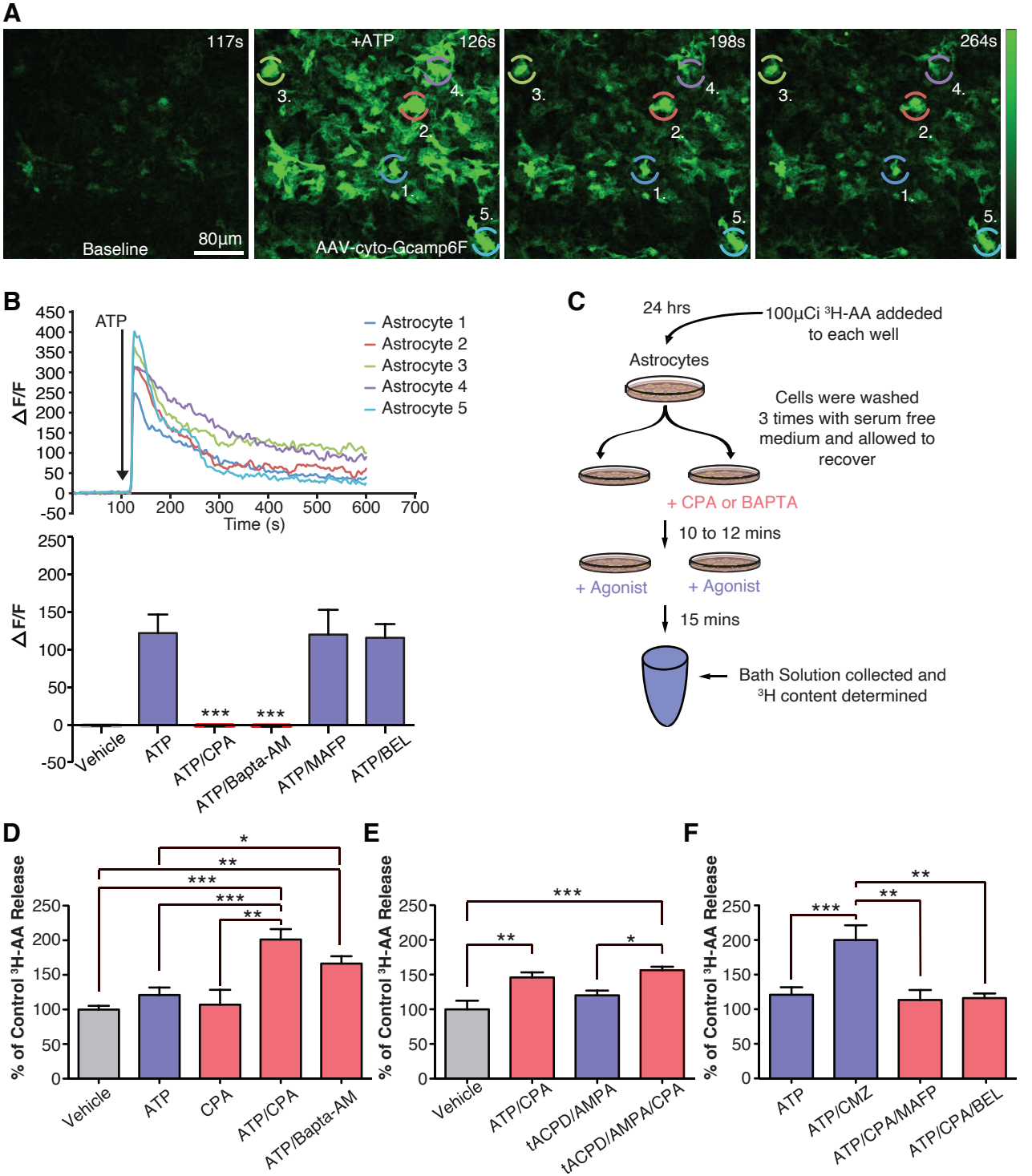
A
117s
+ATP
126s
198s
264s
3.
4.
2.
1.
5.
Baseline
80µm
AAV-cyto-Gcamp6F
B
ATP
Astrocyte 1
Astrocyte 2
Astrocyte 3
Astrocyte 4
Astrocyte 5
Δ F/F
Time (s)
Vehicle
ATP
ATP/CPA
ATP/Bapta-AM
ATP/MAFP
ATP/BEL
C
24 hrs
100µCi ³H-AA addeded to each well
Astrocytes
Cells were washed 3 times with serum free medium and allowed to recover
+ CPA or BAPTA
10 to 12 mins
+ Agonist
+ Agonist
15 mins
Bath Solution collected and ³H content determined
D
% of Control ³H-AA Release
Vehicle
ATP
CPA
ATP/CPA
ATP/Bapta-AM
E
Vehicle
ATP/CPA
tACPD/AMPA
tACPD/AMPA/CPA
F
ATP
ATP/CMZ
ATP/CPA/MAFP
ATP/CPA/BEL

Figure 1

A

Relative differences of lipid levels in astrocytes treated with CPA and ATP compared to vehicle

Prostaglandins	
PGE_2	↑↑↑
Free fatty acids	
Arachidonic acid	↑
Linoleic acid	*n.d.*
2-arachidonoyl-sn-glycerol	
2-arachidonoyl-sn-glycerol	↑
2-linoleoyl-sn-glycerol	*n.d.*
2-oleoyl-sn-glycerol	*n.d.*
-acyl ethanolamine	
N-palmitoyl ethanolamine	↑↑
N-stearoyl ethanolamine	↑↑
N-oleoyl ethanolamine	↑↑
N-linoleoyl ethanolamine	*n.d.*
N-arachidonoyl ethanolamine	↑
N-docosahexaenoyl ethanolamine	↑↑
***N*-acyl glycine**	
N-palmitoyl glycine	*n.d.*
N-stearoyl glycine	↑
N-oleoyl glycine	↑
N-linoleoyl glycine	*n.d.*
N-arachidonoyl glycine	*n.d.*
***N*-acyl serine**	
N-palmitoyl serine	*n.d.*
N-stearoyl serine	*n.d.*
N-oleoyl serine	*n.d.*
N-arachidonoyl serine	*n.d.*
***N*-acyl taurine**	
N-arachidonoyl taurine	↑
***N*-acyl tyrosine**	
N-palmitoyl tyrosine	↑
N-stearoyl tyrosine	↑
N-oleoyl tyrosine	↑
N-arachidonoyl tyrosine	*n.d.*
N-docosahexaenoyl tyrosine	↑
***N*-acyl tryptophan**	
N-palmitoyl tryptophan	*n.d.*
N-oleoyl tryptophan	*n.d.*
N-docosahexaenoyl tryptophan	*n.d.*

Magnitude Differences	
2-2.99 times higher	↑↑↑
1.50-1.99 times higher	↑↑
1-1.49 times higher	↑
Significant Differences	
Significant increase p<0.05	
Significant increase p<0.05-0.10	
no difference between groups	*n.d.*

B

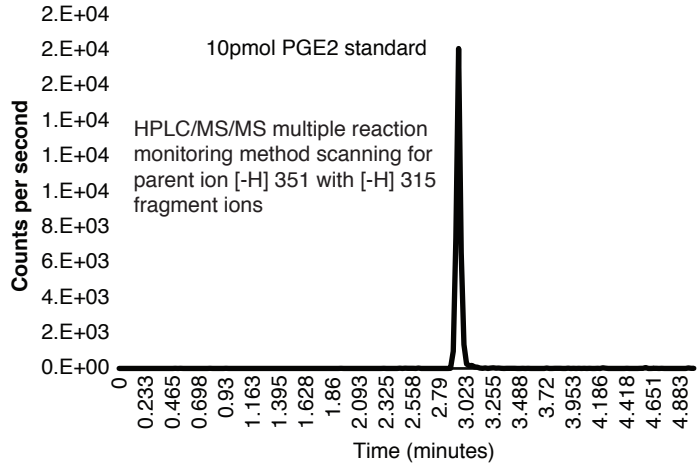

C

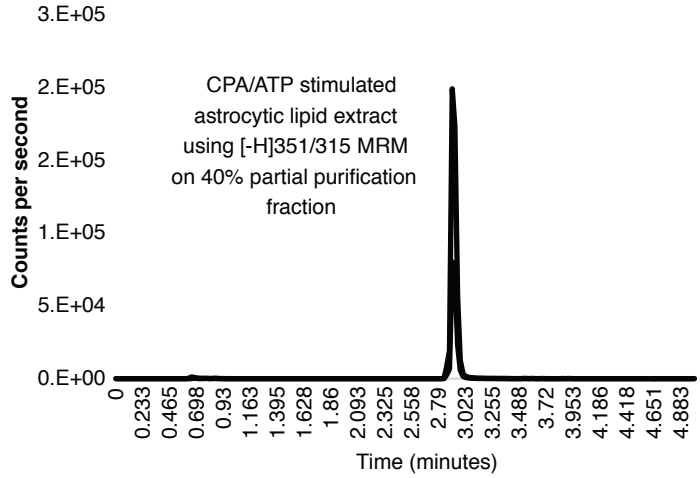

D

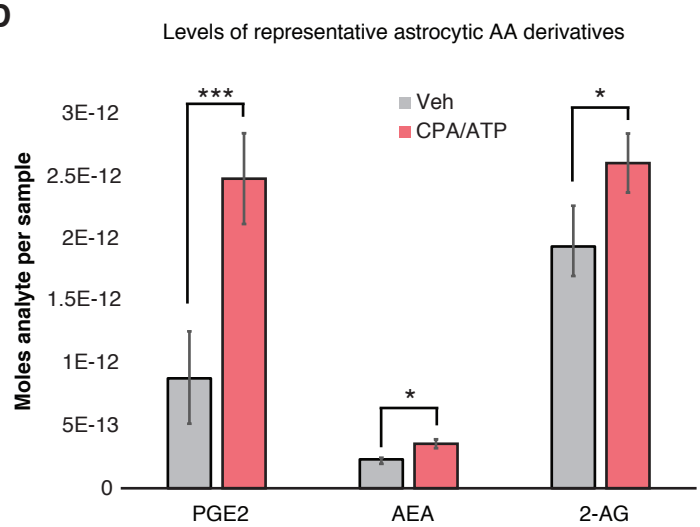

Figure 2

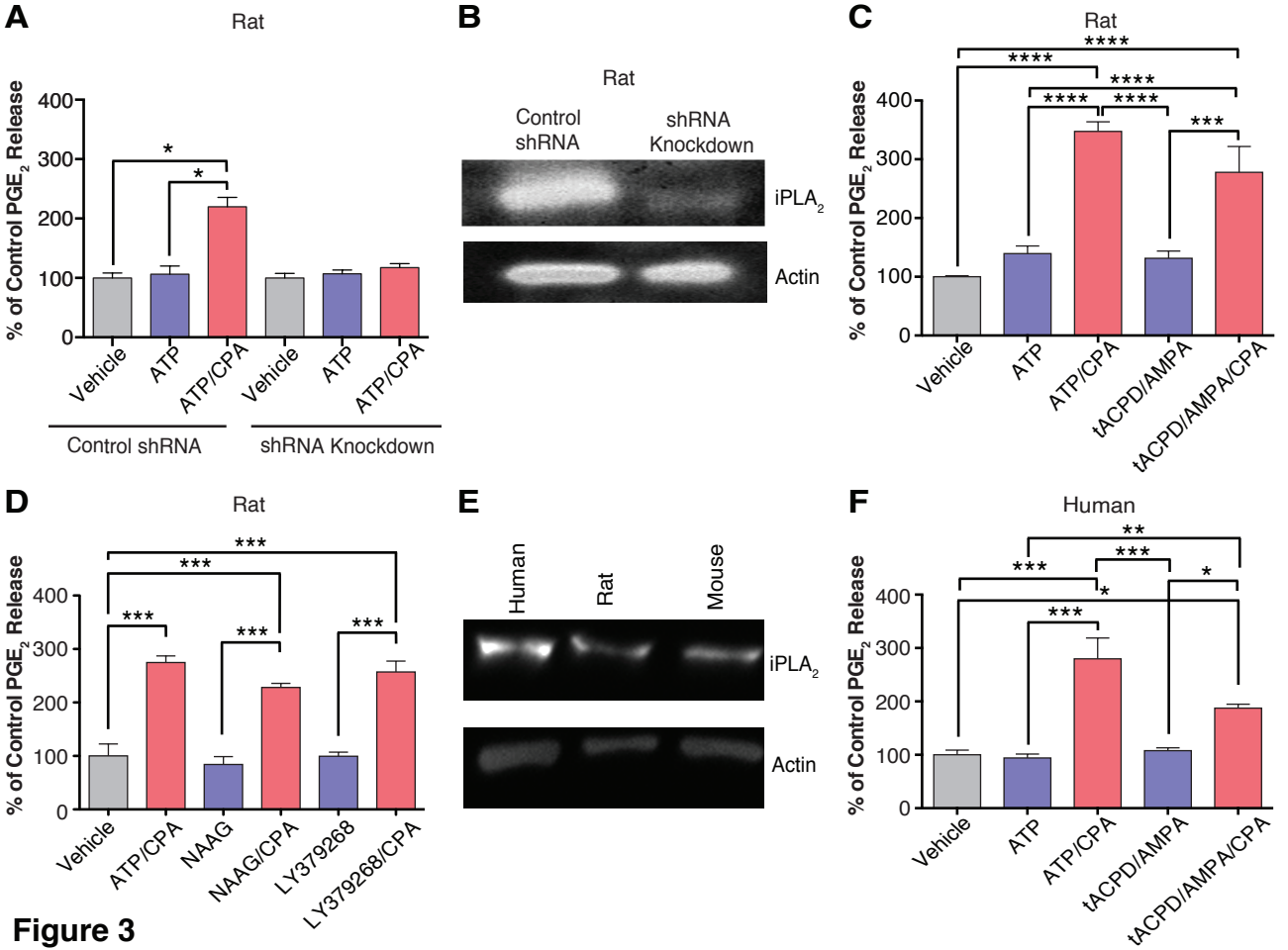
A
Rat
% of Control PGE2 Release
400
300
200
100
0
*
*
Vehicle
ATP
ATP/CPA
Vehicle
ATP
ATP/CPA
Control shRNA
shRNA Knockdown
B
Rat
Control shRNA
shRNA Knockdown
iPLA2
Actin
C
Rat
% of Control PGE2 Release
****
****
****
****
****
***
Vehicle
ATP
ATP/CPA
tACPD/AMPA
tACPD/AMPA/CPA
D
Rat
% of Control PGE2 Release
***
***
***
***
***
Vehicle
ATP/CPA
NAAG
NAAG/CPA
LY379268
LY379268/CPA
E
Human
Rat
Mouse
iPLA2
Actin
F
Human
% of Control PGE2 Release
**
***
***
*
*
***
Vehicle
ATP
ATP/CPA
tACPD/AMPA
tACPD/AMPA/CPA

Figure 3

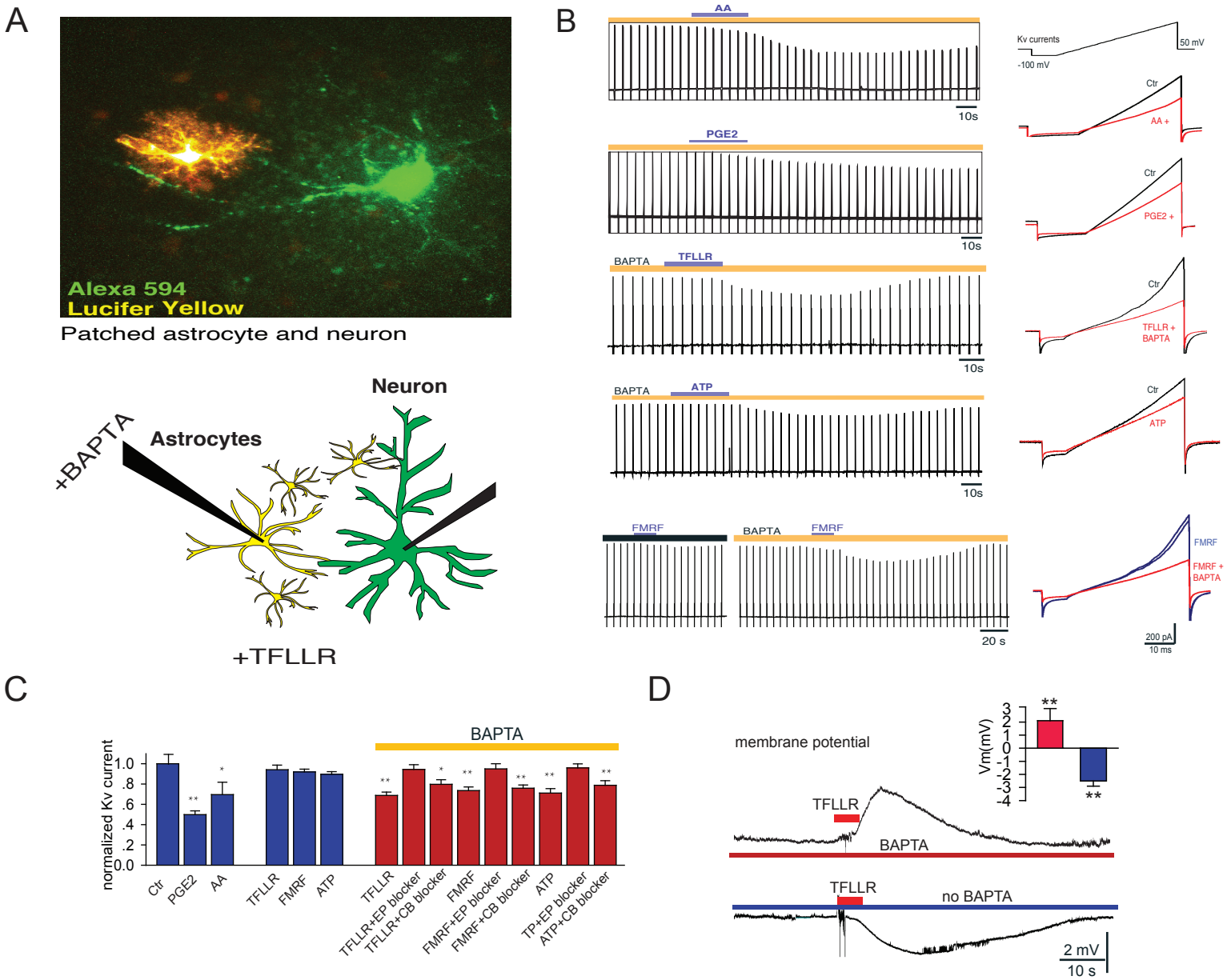
A
Alexa 594
Lucifer Yellow
Patched astrocyte and neuron
Neuron
+BAPTA
Astrocytes
+TFLLR
B
AA
10s
PGE2
10s
BAPTA
TFLLR
10s
BAPTA
ATP
10s
FMRF
BAPTA
FMRF
20 s
Kv currents
50 mV
-100 mV
Ctr
AA +
PGE2 +
TFLLR +
BAPTA
ATP
FMRF
FMRF +
BAPTA
200 pA
10 ms
C
BAPTA
normalized Kv current
1.0
.8
.6
.4
.2
0.0
Ctr
PGE2
AA
TFLLR
FMRF
ATP
TFLLR
TFLLR+EP blocker
TFLLR+CB blocker
FMRF
FMRF+EP blocker
FMRF+CB blocker
ATP
TP+EP blocker
ATP+CB blocker
D
membrane potential
Vm(mV)
3
2
1
0
-1
-2
-3
-4
TFLLR
BAPTA
TFLLR
no BAPTA
2 mV
10 s

Figure 4

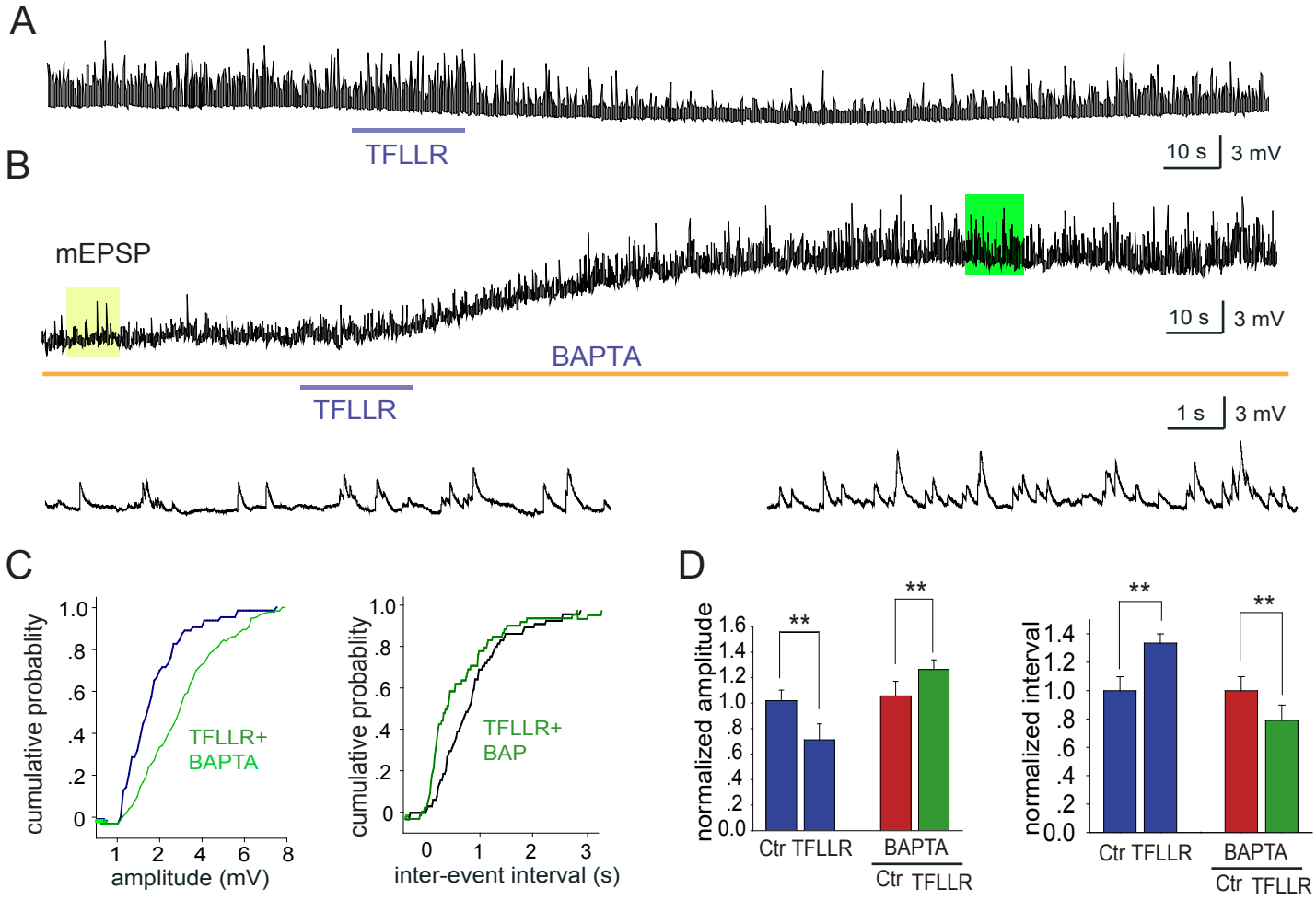
A
TFLLR
10 s
3 mV
B
mEPSP
10 s
3 mV
BAPTA
TFLLR
1 s
3 mV
C
cumulative probablity
1.0
.8
.6
.4
.2
0
1
2
4
6
8
amplitude (mV)
TFLLR+
BAPTA
cumulative probablity
1.0
.8
.6
.4
.2
0
0
1
2
3
inter-event interval (s)
TFLLR+
BAP
D
normalized amplitude
1.6
1.4
1.2
1.0
.8
.6
.4
.2
0.0
**
**
Ctr
TFLLR
BAPTA
Ctr
TFLLR
normalized interval
1.4
1.2
1.0
.8
.6
.4
.2
0.0
**
**
Ctr
TFLLR
BAPTA
Ctr
TFLLR

Figure 5

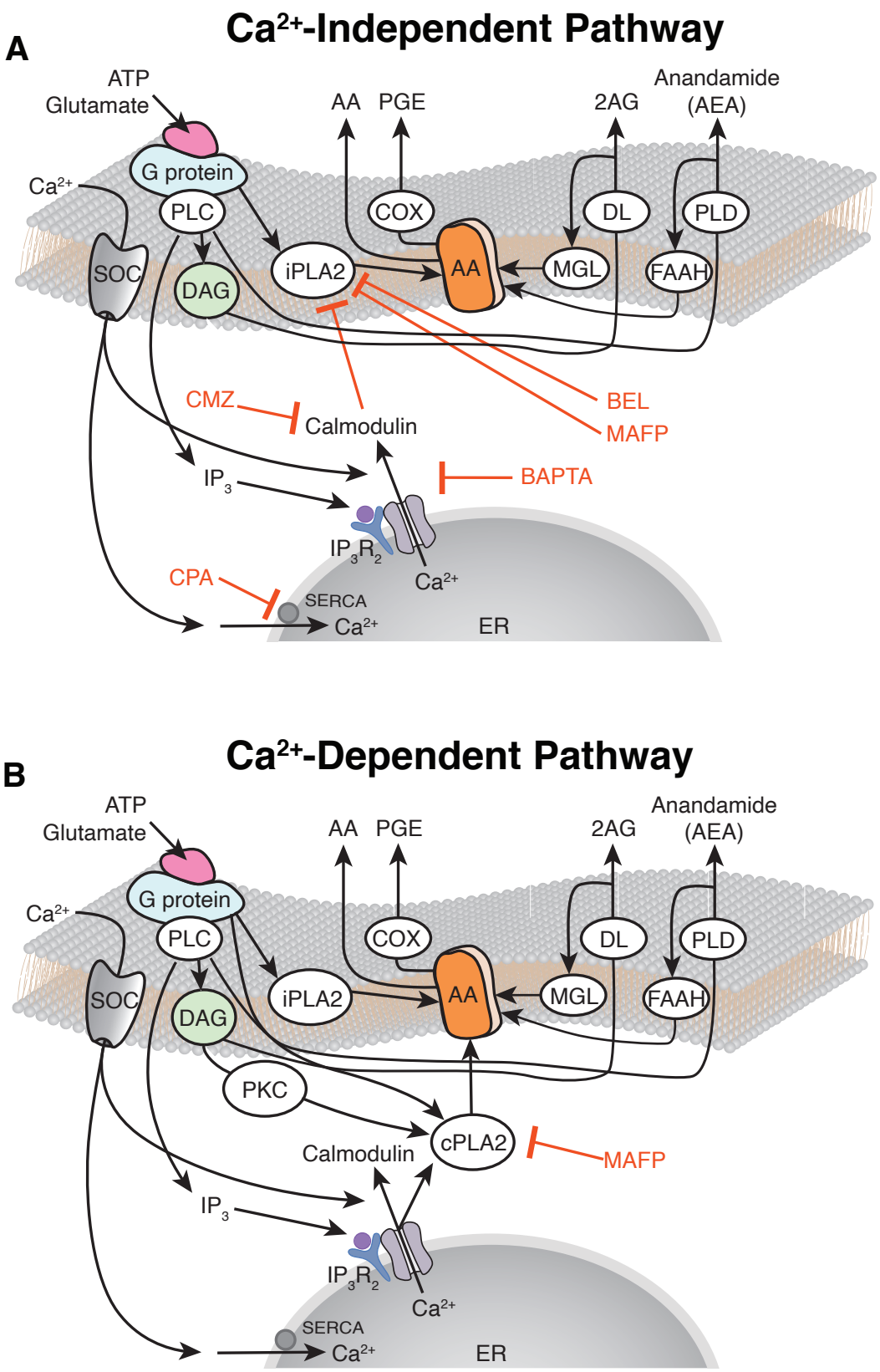
A
Ca2+-Independent Pathway
ATP
Glutamate
AA
PGE
2AG
Anandamide
(AEA)
G protein
Ca2+
PLC
COX
DL
PLD
SOC
DAG
iPLA2
AA
MGL
FAAH
CMZ
Calmodulin
BEL
MAFP
IP3
BAPTA
IP3R2
Ca2+
CPA
SERCA
Ca2+
ER
B
Ca2+-Dependent Pathway
ATP
Glutamate
AA
PGE
2AG
Anandamide
(AEA)
G protein
Ca2+
PLC
COX
DL
PLD
SOC
DAG
iPLA2
AA
MGL
FAAH
PKC
cPLA2
Calmodulin
MAFP
IP3
IP3R2
Ca2+
SERCA
Ca2+
ER

Figure 6